TECHNICAL NOTES

NATIONAL ADVISORY COMMITTEE FOR AERONAUTICS.

No. 204

A STUDY OF STATIC STABILITY OF AIRSHIPS.

By Frank Rizzo,
Langley Memorial Aeronautical Laboratory.

September, 1924.

NATIONAL ADVISORY COMMITTEE FOR AERONAUTICS.

TECHNICAL NOTE NO. 204.

A STUDY OF STATIC STABILITY OF AIRSHIPS.

By Frank Rizzo.

Introduction

The subject matter of this report, submitted to the National Advisory Committee for Aeronautics for publication, deals with the study of static stability of airships and is subdivided into two sections, a theoretical discussion and an experimental investigation.

The experimental work was carried out in the four-foot wind tunnel of the Massachusetts Institute of Technology, and the results were originally submitted by the writer as a thesis in the course in Aeronautical Engineering at that Institution.

The author wishes to express his indebtedness to Professor Warner, head of the Aeronautical Department, for the helpful suggestions during the preparation of the thesis and to Messrs. Ober and Ford of the same department for the valuable assistance received in the performance of the experiments.

Summary

The first section of this work deals entirely with the theoretical side of statical stability of airships in general, with particular reference to conditions of equilibrium, longitudinal

stability, horizontal flight, directional stability, critical speed and a discussion of the reversal of controls.

The second section, besides tests of a preliminary nature on the model alone, comprises experiments for the determination of:

Effects due to change of tail area.

Effects due to change of aspect ratio.

Effects due to change of tail form.

Effects due to change of tail thickness.

In all these tests, longitudinal and transverse forces on the model at various angles of yaw and angles of tail setting were observed and the results and deduction derived therefrom are found in Tables III to IX and Figures 11 to 19.

From the experimental data we may summarize that:

(1) An increase of area over the standard tail surface is undoubtedly advantageous, probably more so for the horizontal stabilizers than for the vertical ones, while a reduction of area would be dangerous.

(2) Similarly an increase of aspect ratio is highly recommended, while a reduction would be unwise.

(3) From the form point of view a rectangular shaped tail surface is far superior to the other two, while the one with balanced rudder is better than the standard shaped one.

(4) The results on the thickness experiments, at least from an aerodynamic point of view, are in favor of the thin-

nest section, tail No. 9 (Fig. 19).

PART I.

THEORETICAL STABILITY OF AIRSHIPS.

Static Equilibrium.

An airship is in static equilibrium when the ascensional force is equal to the total weight, a condition which takes place at an altitude where the weight of the air displaced by the airship is just equal to its total weight. When this condition is fulfilled the center of gravity and the center of buoyancy of the airship lie on the same vertical line and the equilibrium condition is expressed by the formula:

$$W = F = \rho V$$

where ρ is the air density at the altitude in question and V is the displaced volume of air.

From this condition of equilibrium, the airship can ascend or descend only by two distinct causes, namely, atmospheric changes or the discharge of ballast or gas respectively.

Statical Stability of Airships.

An airship in steady flight has three types of stability; that of pitch or longitudinal stability, that of yaw or directional stability, and that of roll about the longitudinal axis. While these stabilities are all correlated in the case of an air-

plane, such, however, is not the case with an airship, the three types of stability being independent of each other. Furthermore, due to the fundamental properties of lighter-than-air craft, static and dynamic stability are both true and distinct, since strictly speaking the only real statical stability is that which exists when the engines are stopped.

An airship is said to be statically stable if it tends to return toward the initial condition of steady motion whenever slightly disturbed from said motion. The above definition applies to motion in which the longitudinal axis of the airship moves on either the vertical or the horizontal plane and the following discussion, applying to these two types of stability, will be based upon these assumptions:

(a) That the ascensional force remains constant.

(b) That the total weight remains constant.

(c) That the speed remains the same.

(d) That the form of the airship remains unchanged.

(e) That the C.G. and C.B. remain fixed.

In actual practice, however, this is never the case; the initial static equilibrium is gradually changing during ascent on account of the adiabatic cooling of the gas and on account of the expenditure of fuel. The center of gravity of the gas moves fore and aft along a line above the longitudinal axis of symmetry, due to the motion of the gas in the inclined position of the envelope. This motion will be forward of the normal position when in an as-

cending attitude and aft when in a descending one. These changes will in turn produce also a slight variation in the aerodynamic moment due to the alteration introduced in its couple arm.

In rigid and semirigid types of airships this inconvenience is to a great extent eliminated by having gas-proof diaphragms of oiled silk at suitable intervals fore and aft; these diaphragms permit the gas to diffuse slowly in case of excess pressure in one compartment over its neighbors, but they are still sufficiently impermeable to prevent the uprush of gas when the airship pitches.

If we take an airship flying along a trajectory which makes an angle θ with the horizontal, and its longitudinal axis makes an angle α with the path, or an angle $(\theta \pm \alpha)$ between the axis and the horizontal, the airship will be in static equilibrium under the action of the following forces and moments (See Fig. 1):

(1) Longitudinal resistance $R = K_1 V^2$

(2) Lift or lateral force $L_e = K_2 V^2$

(3) Pitching moment $M_e = (K_3 V^2)\, l.$

These forces and couples, due to the dynamic reaction of the air, apply for motion of the axis in both the vertical and horizontal planes, in so far as the envelope is a body of revolution and giving as a result equal air reactions for the same inclination of the axis to the wind in pitch and yaw respectively.

In addition to the aforesaid, we also have a moment contributed by the lift of tail surfaces perpendicular to the plane of motion as expressed by:

(4) $M_t = (K_4 V^2)a$

Other forces and couples in the vertical plane are:

(5) The thrust T of the propeller parallel to the axis of the envelope acting c units below the C.G.

(6) The ascensional force F acting upward through the center of buoyancy of the envelope.

(7) The total weight W of the complete airship acting through the center of gravity.

(8) A couple due to the propeller thrust = Tc.

(9) The static righting moment due to the total weight and the inclination of the axis with the horizontal:

$$M_S = Wh\ (\theta \pm \alpha).$$

Longitudinal Stability.

The following conditions of equilibrium must be satisfied for longitudinal stability, when the C.G. is assumed coincident with the C.B. (See Fig. 1).

$$\Sigma H = R + T = 0 \qquad (I)$$

$$\Sigma V = F \pm L_e \pm L_t - W = 0 \qquad (II)$$

$$\Sigma M = Tc \mp L_t a \pm M_e = 0 \qquad (III)$$

Horizontal Flight.

With the ship on an even keel ($\theta = \alpha = 0$), and on further assumption that $F = W$

Then, $L_e \pm L_t = 0$

and, $M_e + L_t a + Tc = 0 \qquad (IV)$

Observing that the static moment is zero, and that M_e and L_e act always in the same direction, one of three possible conditions may exist:

(a) If M_e and $L_e = 0$, then T_c is left unbalanced.

(b) If M_e and L_e are positive, L_t is negative and the airship would be unstable under the action of three couples all acting in the same direction.

(c) If M_e and L_e are negative, L_t is positive and $T_c = M_e + L_t a$.

This proves that the airship can maintain static equilibrium in horizontal flight only when the above condition is satisfied, namely, by flying with a small negative angle of incidence and the cooperation of the control surfaces.

In general, however, when $\theta \neq 0$ and the C.G. is below the C.B., equation IV becomes:

$$M_e + L_t a + T_c - Wh\theta = 0$$

for all angles and the general equations become:

(1) $F\cos(\theta \pm \alpha) - W\cos(\theta \pm \alpha) = L_e + L_t$; normal to path.

(2) $R \pm W\sin(\theta \pm \alpha) = T \pm F\sin(\theta \pm \alpha)$; parallel to the path.

(3) $T_c \pm Wh(\theta \pm \alpha) \quad M_e \mp M_t = 0$; about C.B. of envelope.

Again, at the altitude where $W = F$

equation (1) gives $L_e = -L_t$

also if α is zero, $L_e = 0$

and $L_t = 0$

which condition, when applied to equation (3) gives:

$$Tc = 0$$

This is an impossibility as long as the airship is under way, since from equation (2) T must at least balance R and is invariably acting at a distance c below the center of buoyancy. The only alternative left is that some pitching moment must be preserved to counteract the thrust couple Tc. This, in practice, is accomplished by the tail surface couple $L_t a$; L_t is in turn balanced by L_e, which force introduces also a negative envelope couple M_e, and the above conditions of equilibrium are thus reestablished providing that $(\theta \pm \alpha)$ does not become zero. For values of $(\theta + \alpha) > 0$, and $F = W$, then we get:

$$L_e = -L_t$$

$$T = -R, \text{ and}$$

$$(4) \qquad Tc + M_e = Wh\,(\theta + \alpha) \pm L_t a$$

If, however, $(\theta + \alpha) < 0$, the latter condition becomes:

$$(5) \qquad Tc + Wh\,(\theta - \alpha) = M_e \pm L_t a.$$

That is, the static couple $Wh\,(\theta \pm \alpha)$, works against the thrust couple in a climbing attitude of the ship and with it in a descending attitude. The reverse is true concerning the envelope pitching moment M_e; it helps to keep the nose of the airship in a climbing attitude in the former case and vice-versa when $(\theta + \alpha) < \theta$.

To be sure, in horizontal flight both M_e and $Wh(\theta \pm \alpha)$ disappear as α approaches zero; under any other conditions, however, while both moments are straight line functions of α, the envelope moment M_e varies also with the second power of the speed.

A study of the above general equations of equilibrium indicates that the airship is most unstable at zero angle of incidence; it indicates also that any excess or lack of ascensional force must be balanced by dynamic load, requiring that the airship must fly at such an angle of incidence as to satisfy the condition on hand. In the particular case when $W > F$, an equivalent amount of ballast must be disposed of if the engines should stop in order to maintain equilibrium; and vice-versa, when $F > W$, an equivalent amount of gas must be valved out if the engines should stop in a dynamic descent.

Directional Stability.

If the above airship flying in longitudinal equilibrium is caused to turn about its vertical axis by a certain deviation of the rudder the resulting motion will be circular in a horizontal plane and new forces and moments will appear which are, with the exception of the centrifugal force, identical with those dealt with in the longitudinal stability.

Looking at it from a different point of view, since the airship is now moving in a curved path the unbalanced forces acting on it may be resolved into tangential and normal components; the

tangential component will be:

$$F_t = \frac{Md^2s}{dt^2}$$

and the normal component

$$F_n = \frac{MV^2}{r} = \frac{M}{r}\left(\frac{ds}{dt}\right)^2$$

where r is the instantaneous radius of curvature of the path determined by the intersection of perpendiculars to the instantaneous trajectories of any two points on the airship. It is obvious then, that as far as the forces in the horizontal plane are concerned, the centrifugal force due to yaw and the thrust must be in equilibrium with the resultant air force, or

(I) : $Y_e + Y_t + T \sin\psi + C.F. = 0$, normal to path.

(II) : $T \cos\psi + R = 0$, parallel to path.

and (III): $N_e + N_t + T\,(c \sin \Phi) = 0$, in yaw.

Where T is the thrust when the longitudinal axis inclines ψ° with the path and the Z axis Φ° with the vertical; $c \sin\Phi$ is the arm of the new thrust couple in the horizontal plane, c being, as before, the distance between the center of buoyancy and the line of thrust.

In a way similar to that of longitudinal stability N_e and Y_e must be both negative; and since Y_t must of necessity have the same sign as the centripetal force, to insure negative N_e the angle of incidence must be negative (inside of the trajectory) and the rudder setting β also towards the concave side of the path.

Critical Speed of Airships.

If the airship in question, maneuvering at a speed V with the controls in neutral position, were left free while in motion with its axis along the trajectory, it would take a drift angle of about 20 degrees in yaw*, and the yawing moment causing this drift is, in practice, counterbalanced by the control in the vertical plane, the rudder.

In the case of pitching motion the dynamic reversing moment is partially counterbalanced by the righting moment contributed by the total weight W at the C.G., h feet below the C.B.

It is evident then, that if we take the above airship in straight flight without tail surfaces, longitudinal static stability is only possible as long as the static uprighting moment is greater than the dynamic upsetting moment in pitch,

$$\text{that is, } : M_s > M_e$$

$$\text{or : } Wh\theta > KW\theta V^2$$

where h is the distance of the C.G. below the C.B. and θ the angle which a vertical in the plane of symmetry makes with the line joining these two points.

Since the left member is fixed for a given angle of pitch, and the right member varies with the square of the speed, there will be a velocity V beyond which, without the assistance of elevators, the airship would become unstable; this is the so-called critical

* Hunsaker, Smithsonian Miscellaneous Collections, Vol. 62, No.4.

speed of the airship and expressed by

$$V > \sqrt{\frac{h}{k}}$$

If we now apply tail surfaces to the envelope, the value of K being a linear function of the tail surfaces involved, and h surely being proportional to the linear dimension of the envelope, it can be easily inferred that if such large area could be used as to make K approach zero, V would become infinity; this is only theoretically possible, as various mechanical reasons would prohibit the use of both the enormous tail area and the great speed as well.

Rate of Control Motion.

If the controls of an airship under way are suddenly shifted from an original setting θ_1 to θ_2 in a short interval of time, the air force acting on its surface is no longer that due to the speed V of the airship, but to W the resultant velocity of V and of U the velocity due to rotation of the surface about its instantaneous center, the hinge.

That is,

$$W = \sqrt{V^2 + U^2}$$

where

$$U = l_1 \left(\frac{d\theta}{dt}\right)$$

and l_1 is the radius of gyration of the moving surfaces. The dynamic force due to this rotational speed U is

$$R = K_1 A U^2 = K_1 A l_1^2 \left(\frac{d\theta}{dt}\right)^2$$

and the corresponding couple about the hinge is:

$$C_1 = K_1 A l_1^3 \left(\frac{d\theta}{dt}\right)^2$$

while that due to the translational speed is:

$$C_2 = K_2 A V^2$$

The combined effective couple about the hinge is therefore the summation of these:

$$C_r = C_1 + C_2$$

This resultant couple causes the airship to turn with an angular acceleration around a pivoting point P (Fig. 2), so that any portion of it, at a distance l_2 from P, and of area A, will have

a velocity through space of $l_2\left(\frac{d\theta}{dt}\right)$

an aerodynamic force of $A\,(l_2^2)\left(\frac{d\theta}{dt}\right)^2$

and a moment about P proportional to $A\,(l_2^3)\left(\frac{d\theta}{dt}\right)^2$

opposing the angular motion of the airship about point P.

The angular acceleration is not, and ought not to be very large due to the enormous inertia of the airship; the retarding moment, on the other hand, which is zero at the start, increases to a maximum when it is equal to the couple C_r and the ship has reached uniform angular motion and finally dies out as soon as the control couple C_r is dissipated.

The outstanding feature of this retarding moment is that it

varies as the square of the angular speed, but what is more important, as the cube of the distance l_2. This distance l_2 is moreover subject to great change, as the point P, for a given curvilinear path, moves forward of the center of buoyancy with increasing angle of yaw. Recent free flight experiments on a C-class airship* by the National Advisory Committee for Aeronautics, have indicated that the axis of the angular motion P moved as far forward as the nose. Little is known so far concerning the total resistance to transverse motion or to turning; whatever the nature and distribution of this force, we are safe, however, in stating that the effect of these transient couples on airship hulls is considerably more serious when the controls are moved from one extreme position to the other of the vertical plane of symmetry, due to the fact that the stresses thus incurred are all reversed. The danger of exceeding the maximum allowable stresses is undoubtedly most pronounced in the case of nonrigid and of semirigid airships in which the envelope has to stand stresses due to internal pressure and to bending moments as well. These facts indicate the militant necessity of keeping the angular acceleration of airships within allowable limits so that their enormous inertia coupled to the great distance of tail surfaces from the instantaneous center of rotation may not give cause to such disastrous results, as those of which the R-38 was probably a victim.**

---

* Report No. 208, "A Determination of Turning Characteristics of the C-7 Airship by Means of a Camera Obscura."

** The British Aeronautical Committee, upon the causes that contributed to the destruction of the airship R-38, says: "The structure was not improbably weakened by the cumulative effect of reversals of stresses of magnitude not far short of the failing stress." (Aerial Age, March 6, 1922.)

PART II.

Description of Model Used.

A model airship of the L-33 type was constructed by the author according to dimensions previously used by the British Advisory Committee for Aeronautics.*

The model, 1/153 of the full size, with an overall length of 50.6" and a maximum diameter of 6.2" was built in two halves of 7/8" laminae, hollowed out before assembling, so that the weight could be reduced to a minimum. The odd dimension of 1/153, instead of 1/150 the full size, as previously planned, is purely accidental, being caused by six months of extra seasoning.

Drawings and characteristics of the airship model are shown in Fig. 3, and the lines tabulated in Table Ia. Tail units 1 to 9 inclusive, are indicated in figures following the model. These tails are all made of white wood with the exception of set No. 9, which is only 1/16" thick and consequently made of aluminum plate.

Tunnel and Apparatus.

The experiments as previously stated were made in the 4-foot wind tunnel of the Massachusetts Institute of Technology, the 8-foot one being still under construction at the time. A detailed description of the wind tunnel has been given by Professor Warner in "Aviation," of March 13, 1922, and needs no repetition here. The airspeed was 40 M.P.H. for all tests and calibration of this had

* R&M No. 361.

previously been checked by means of a Chattock gage.

The Balance.

An attempt was made to use the N.P.L. balance available but the weight of the model (approximately 9 lb.) was so great that it raised the center of gravity of the whole system and caused the balance to become sluggish and insensitive. It was therefore decided to use a wire suspension balance of the Göttingen type diagrammatically shown on Fig. 4.

The use of this type of balance incidentally has two advantages over the ordinary method of suspending the model on a spindle. First, the results are more accurate, since the elasticity of the spindle causes the model to vibrate and accurate readings are thus rendered very difficult, while with the suspension balance the vibrations are eliminated and the difficulty removed. Secondly, due to the definite location of the wire attachments on to the model, the position of the resultant force is readily determined, while in the spindle type of balance this determination can only be obtained in an indirect way.

Disadvantages, which are, however, common to both types of balance are: sluggishness under heavy models and marked vibrations at angles of pitch greater than 10°, especially when the control surfaces are set at large angles.

Referring to Fig. 4, the airship model is counterweighed by weights w_1 and w_2. The fine wires a and b engage with balances

A and B respectively. Wires c and d meeting at o connect to balance C. Wire e has its lower end fixed to the floor of the tunnel and makes an angle of 45° with it.

Counterweight w_3 serves to keep the apparatus in tension thus preventing any undesirable motion and unnecessary vibrations of the suspended model.

From what precedes, it is clearly seen that the dead weight of the model is taken care of by the counterweights w_1 and w_2 and that the balances A and B carry the vertical component of the dynamic load, corresponding to the crosswind force or lift; similarly, since wires c and d are flexible members capable of taking tension only, and since wire e makes equal angles with c and d, the pulls in these must be equal to each other and balance C therefore carries the resistance in the line of flight, or the drag.

The inclination of the model was adjusted by sighting through a protractor alongside of the tunnel on to the axis of the envelope, care being taken that the drag wire remained horizontal at all angles of pitch. The angles were set once and for all by means of engaging nuts fastened along wires a and b, one pair for each angle setting; the wire d was kept horizontal by properly locating the suspension pulleys f and g simultaneously to the proper adjustments.

Resistance of Wire Balance.

The best way to determine the resistance due to the wire of

the balance would have been by doubling on all wires, care being taken that no additional drag due to interference is introduced by the second set of wires. The extra drag introduced by the latter would then have corresponded to the wire drag and mutual interference of the model and wire balance proper. The precision of the balance as a whole did not, however, warrant such refined precision and resort was therefore made to an empirical determination of this balance drag.

The balance was so rigged that the model hung in the middle of the tunnel when at an angle of 20° with the horizontal, the drag wire remaining always parallel to the wind direction, and that portion of wire between stern and rearward counterweight varied from horizontal to plus or minus 10° inclination. The resistance of the wire in each case was figured on that part of the wire subjected to the action of the airstream between model and tunnel wall. This was done for each attitude of the model and was deduced from available experiments* on wire, the interference between model and balance was disregarded in all cases.**

---

* R&M Nos. 102 and 307.

** This fact is partly justified by previous experiments on similar tests, in which, approaching the model by a wire three times as thick as that used for the suspension introduced, no appreciable change in the resistance (R&M No. 244, p.42).

Balance Resistance.

TABLE I.

α°	l' cm	Res. g	$\frac{l'/2+42}{l'+42}$	R' g	l" cm	Res. g	$\frac{l''/2-42}{l''-42}$	R" g	R g	Total resist. g
0	76.2	11.3	.791	9.0	76.2	11.3	.791	9.0	18.0	19.0
5	74.4	11.0	.795	8.8	67.8	10.2	.798	8.0	16.8	17.8
10	72.6	10.8	.797	8.6	59.2	8.8	.830	7.2	15.8	16.8
15	70.8	10.5	.799	8.2	49.8	7.4	.838	6.2	14.4	15.8

In the preceding table, the intercepted length l' and l" of the forward and rear wire suspension respectively, are, in each case, multiplied by the resistance of the wire per unit foot (3.76 g) and entered in columns 3 and 7 respectively. The factors

$$\frac{l'/2 + 42}{l' + 43} \quad \text{and} \quad \frac{l''/2 + 42}{l'' + 43}$$

are the proportions of these resistances carried by the drag balance (See Fig. 4). Taking the drag of the longitudinal wires (practically constant for all attitudes of the model in the wind tunnel) as .08 g per foot and adding it to R' and R" we get the total drag of the wire balance for each attitude of the model, shown in the last column of the above table.

Envelope Resistance.

The absolute coefficients C_1 and C_2 per unit area and unit volume respectively, the resistance R, the airspeed v, and the

density of air (2.37×10^{-3} slug/ft.^{3}), the volume V and the maximum cross-sectional area A of the airship are related by the formulas:

$$R = C_1 \rho A v^2$$

and $$R = C_2 \rho V^{2/3} v^2$$

R in both cases being corrected for the spurious force on the model due to the drop in static pressure along the axis of the tunnel.

Pressure Drop Correction.

The pressure gradient for this particular tunnel is represented, at any speed, by the equation:

$$p = -.000045V^{1.88}$$

where p is the drop in static pressure in pounds per square foot per foot of run along the axis of the tunnel, and V the velocity of wind in miles per hour.

Taking the volume of the model as 0.579 ft.^{3}, and 40 M.P.H. for V, we obtain the total pressure drop correction to be deducted from the total drag to be

$$F = pv = 0.043 \text{ lb.}$$

Dimensions of "33" Class Airship Model.

TABLE Ia.

Station	x/D	d/D	x(in.)	D(in.)
1	0.0	0.0	0.0	0.0
2	0.042	0.184	0.184	1.160
3	0.208	0.415	1.310	2.620
4	0.354	0.536	2.230	3.380
6	0.687	0.719	4.330	4.530
8	1.080	0.854	6.800	5.370
10	1.490	0.943	9.400	5.950
12	1.910	0.988	12.02	6.230
14	2.325	1.000	14.65	6.30
18	3.160	1.000	19.90	6.30
23	4.210	1.000	26.65	6.30
25	4.630	0.991	29.20	6.25
27	5.040	0.962	31.70	6.16
29	5.460	0.907	34.40	5.71
31	5.860	0.831	37.00	5.24
33	6.280	0.737	39.60	4.65
35	6.710	0.623	42.40	3.93
37	7.120	0.489	44.90	3.08
39	7.530	0.329	47.50	2.08
41	7.900	0.158	49.80	0.99
42	8.050	0.076	50.70	0.48
43	8.170	0.000	51.50	0.00

x = distance from nose

d = diameter

D = maximum diameter

FULL SIZE L = 196.18 meters (643.6 feet)

D = 24.0 meters (78.7 feet)

SCALE OF MODEL: = 1/153

l = 4.22 ft. (50.6 in.)

d = 0.516 ft. (6.2 in.)

Volume = 0.579 ft.^{3}

Center of buoyancy at 47.4% of l

C.B. to C.P. of tail surfaces = 23.25 in.

Significant Characteristics of Tail Surfaces.

Tail surfaces, whether applied to submarines, airplanes or airships perform exactly the same function, that of controlling and steadying the motion of the craft to which they are attached. Water vessels having two or more screws have at times been steered by the propeller alone, but up to the present time no other device has succeeded in superseding the old system of tail surfaces in guiding the vessel in its motion through the medium.

In the case of aircraft, as well as in the case of submarines, due to the three dimensional freedom of motion of these crafts, the problem of controllability becomes very important. The two main questions encountered in the design of control surfaces are:

(a) What moment should the controls produce; and

(b) How efficiently is this moment produced?

The quantitative question in itself is a simple problem in statics, the simplest case of which arises when the airship is travelling with its axis nearly parallel to the trajectory, in which case very little assistance is needed from control surfaces.

If, however, the body AB, moving in the direction of its axis has its rudder moved through a small angle DAC or β, the dynamic pressure acting on it normally to AC is, as shown in Fig. 5,

$$P = ksV^2$$

where k for symmetrical sections similar to the Göttingen* No.429

* N.A.C.A. Reports Nos. 93, 124 and 182: "Characteristics of Airfoils."

or the Eiffel No. 56, is a straight line function of the angle up to 11° and 15° respectively.

This force can be resolved at the hinge into two components: one parallel to AB, and the other perpendicular to it. The force BA tends to retard the motion of the airship while the force AF, by introducing two other forces equal and opposite to it at the C.G. of the body, can be replaced by a couple lF, producing rotation of AB about the C.G., and a force F', tending to move the vessel laterally in the direction of the force. Thus, knowing the speed of the airship through the air, l the distance from O to the center of pressure of control surfaces of area S, we obtain for the rotational moment about O

$$M = k_1 SV^2 l$$

from which it is clearly seen that the only variables involved are the area S and the distance l, both admitting variation within constructional limits.

An airship is most efficiently handled when it takes a small helm to keep it on its course, that is, when it responds readily to control motion; for, if equilibrium is not established in time the lateral motion caused by the unbalanced force F' (Fig. 5) is still further altered by the reaction of the air at the lateral center of pressure of the airship while the center of gravity persists travelling in the original direction; the result is that the angular motion will increase or decrease depending on the location of the center of resistance; if the center of lateral resistance

is back of the center of gravity the direction will be restored, but the swing will be increased on the contrary, hence the cooperation of tail surfaces.

What precedes demonstrates in general the importance of having large fin surfaces and as far back of the center of volume as possible, if other limitations had not to be contended with, namely, the total weight allotted to this item consistent with the economic performance of the aircraft. Nobile*, for example, estimates the weight of vertical planes to be proportional to the surface of the envelope, and the horizontal ones to be proportional to the volume. On this assumption he deduces the total weight of these in terms of the airship volume (M^3) to be:

$$W = (.043)V \text{ kg for empennage,}$$

$$\text{and } W = (.004)V \text{ kg for rudders.}$$

The question of neutralizing the lateral force by means of tail surfaces is most pronounced in the case of an airship flying in a circular path, in which case, in addition to the lateral component of the rudder, we also have to counterbalance the centrifugal force $\frac{m V^2}{r}$ acting in the same direction and through the C.G. of the airship. And since constant angular velocity contributes neither resultant force nor moment**, the only alternative left is to navigate the vessel at such an angle that the transverse dynamic force just neutralizes these lateral components.

* "Giornale del Genio Civile," Anno LIX, 1921.

** N.A.C.A. Technical Note No. 104, on Aerodynamic Forces, by Munk.

This is accomplished by flying the airship so that the cross-wind force is in opposition to the centrifugal force, that is, with its nose inside of the trajectory. The theoretical value of this angle, as deduced by Dr. Munk* is:

$$\alpha \sim \frac{a\,(l)}{R(k_2 - k_1)}$$

in which k_1 is the additional longitudinal mass, and k_2 the additional transverse mass. Taking these mass coefficients as deduced by Lamb** for ellipsoids, for the fineness ratio 8 to be .029 and .945 respectively, then their difference is equal to .916 and the value of α becomes proportional to

$$\frac{a}{R}\left(\frac{l}{.916}\right)$$

where a is the arm of the reversing moment and R the radius of curvature of the trajectory.

Crocco's Coefficient.

When the airship is deviated from its course by an angle α, a reversing moment is produced which will tend to deviate the airship still further unless some external force is applied to produce an equal and opposite couple. This is accomplished by the control surfaces which must be set at an angle α'. The ratio $\frac{\alpha'}{\alpha}$ is then a measure of the efficiency of the control surfaces and the information derived therefrom is that the smaller this ratio is the

* N.A.C.A. Technical Note No. 104, on Aerodynamic Forces, by Munk.
** R&M No. 623, "The Inertia Coefficients of an Ellipsoid Moving in Fluid."

larger the efficiency of the control surfaces in question becomes.

Description and Disposition of Tail Units.

Figs. 9 to 12 inclusive, show dimensions and form of nine tail units used, detailed characteristics of same being given in Table II. They are all streamlined with the maximum thickness at approximately 40% of the chord.

These tail units were so disposed on the airship model that the center of figure of each stabilizing surface was at a distance of 23.25 inches from the center of buoyancy or 47.25 inches from the nose.

The movable parts were attached to the fins by steel wires so that they could be bent and thus set at any desired angle with reference to the fins; only two controls from each set were so fitted, those perpendicular to the plane of inclination, the other two controls having been left integral with the fins.

The above disposition of tail surfaces is justified in part by the fact that the center of pressure travel for similar symmetric sections is the same for angles of pitch or yaw when the controls are in neutral position.

Stabilizing Surfaces.

TABLE II.

Tail No.	Total area	Fixed area	Movable area	Aspect Ratio	Area in % of 1	Maximum thickness in.	Control form	Remarks
1	8.48	6.58	1.90	2.61	100	7/16	Standard	
2	6.56	5.12	1.44	2.61	75	7/16	"	Area
3	12.15	9.29	2.84	2.61	150	7/16	"	group.
1	8.48	6.58	1.90	100%	A_S	T_S	Standard	Aspect
4	8.48	6.58	1.90	75%	A_S	T_S	"	Ratio
5	8.48	6.58	1.90	150%	A_S	T_S	"	group.
3	12.15	9.29	2.84	R_S	150	7/16	Standard	Thick-
6	12.15	9.29	2.84	R_S	150	1/4	"	ness
7	12.15	9.29	2.84	R_S	150	1/16	"	group.
1	8.48	6.58	1.90	R_S	A_S	T_S	Standard	
8	8.95	6.73	2.22	115% R_S	106	T_S	Bal.Rud.	Form
9	8.40	6.48	1.92	99% R_S	99	T_S	Rectang.	group

Note.- Tail surface No. 1 is the standard adopted, as used on the original airship; tail surface No. 3 was, however, used in the third group, instead of No. 1, with the hope that the larger area may help to magnify the presumed minute effects caused by changing the thickness.

Determination of Drag, Lift, Moment and Center of Pressure.

Referring to Fig. 4, showing the model in equilibrium under the action of the forces indicated, we have:

$$\text{Lift} = R_A + R_B$$

$$\text{Drag} = R_C$$

$$\text{Moment}_o = xR_A + zR_C - yR_B$$

Where M is the moment about the center of buoyancy of the model due to the external forces and tending to deviate the airship from its course, drag and lift are the forces parallel and perpendicular to the direction of the airstream respectively, while R_A, R_B and R_C are the forces measured by the balances A, B and C respectively.

The center of pressure through which the resultant R acts is then found by ordinary statics. Thus the resultant force is:

$$R = \sqrt{L^2 + D^2}$$

the angle $$\alpha = \tan^{-1} L/D$$

and the point of application is at a distance a from the chosen axis as given by

$$\Sigma \frac{M}{R}$$

The above determinations apply to all tests in general; those tabulated for each tail surface, however, were obtained by subtracting the forces due to the model alone from those due to model with fins attached.

Similarly, by deducting the moments about the C.G. with elevators in neutral position, from the corresponding moments with elevators set at various angles, we obtain the moments due to the controls themselves. Since the stabilizing surfaces were symmetrically disposed, that is, equal fins and equal controls in both longitudinal planes, and since no cars were used in the investigation, these moments can be taken either for rudder settings or

and angles of yaw, or as elevator settings and angles of pitch.

It must be noted here that if the resultant dynamic forces were plotted relatively to the model at various angles of yaw, we would find that they would describe an envelope with its apex on the axis of the airship.*

From simple static considerations it is evident that the ideal position for this apex would be the center of buoyancy of the envelope of the airship. This condition, however, would require so much fin area as to render the airship over-stable, an undesirable and impracticable condition since a certain amount of instability is desired for the sake of good maneuverability.

Precision of Results.

The results found, even after corrected for pressure gradient, still remain subject to a variety of errors, the most conceivable of which are the following:

(a) Effects due to unsteadiness and turbulence of airstream in the wind tunnel.

(b) Effects due to limited dimensions of the airstream; in this particular case the section of the test chamber (4 ft. dia.) is only 64 times that of the model (1/2 ft. dia.)

(c) Effects of boundary walls of tunnel.

(d) Probable geometrical dissimilarity due to greatly reduced model proportions.

(e) Improper correction for supporting apparatus.

(f) Doubtful machanical similitude between model

* "Theoretische und Experimentelle Untersuchungen an Ballon Modellen" by Fuhrman.

and full-scale airship in the relative motion of the air past the model and past the full-scale airship.

Sources of error (a) and (c) can be corrected for, to a fair degree of precision, by proper estimation of the airspeed around the model region for any particular attitude of the model. Source (b) comes as an effect on the wind speed in the tunnel due to the presence of the model in the channel. As an illustration of the magnitude of this error British investigators have found that with the model at 0° and 5° incidence, for a wind of 40 ft./sec., the values of V^2 varied between -1% and -3% for the lower angles, but for the 5° angle they found it to vary as much as -3% to -8%.

All the above mentioned errors, with the exception of the pressure gradient correction, even though they are of a commensurable nature, are nevertheless not likely to seriously affect the main purpose of the investigation and are therefore considered beyond the object of this research.

Discussion of Results.

The most important feature shown by the test on the model, without stabilizing surfaces, is the low resistance at zero angle of yaw, namely, 51 g (1.8 oz.), giving coefficients:

$$C_1 = R/\rho\ A\ V^2 = \frac{51}{454} \Big/ .002373\ \frac{(\pi)}{4}\ \frac{(6.2)^2}{144}\ \frac{(40 \times 4.4)^2}{3} = 0.0655$$

$$C_2 = R/\rho\ v^{2/3}\ V^2 = \frac{51}{454} \Big/ .002373(.579)^{2/3}\ \frac{(40 \times 4.4)^2}{3} = 0.0198$$

Full line curves on Figs. 6, 7 and 8 are the characteristic curves for the model without stabilizing surfaces; angles of yaw being taken for abscissae, drag and lift, and moments about the C.B. as ordinates; the forces have been plotted in grams as taken from actual observation, and the reversing moments derived therefrom are in lb.-in. units.

The curves show that the drag gradually increases from a minimum at 0° to 171% in 15° of yaw.

The lift curve shows a positive increasing slope up to 10° of yaw and a decrease from there on, with a probable maximum lift somewhere between 25° and 35° of yaw. The reversing moment curve appears to have reached its maximum value at 15° of yaw.

Area Group.

From the performance curves of this group of tail surfaces representing the standard area, 150% A_S and 75% A_S respectively, we observe that the lift in all cases varies, as we may expect, with the area of the tail units, and gradually increasing with the angle of yaw. Tail No. 2, for example, with the controls at 30° and an angle of yaw of 15° furnished as much as twice the lift of the model alone, while the smallest furnishes only 100% L_m at the same conditions.

The reversing moments are almost straight line functions for tails Nos. 1 and 3 when the respective controls are in neutral position; tail No. 2 of this group, however, is slightly convex

upward with a maximum value at 11° of yaw.

As the angle of tail setting increases all the reversing moment curves become convex upward with an initial amount varying from 0 to 5.8 lb.-in. for the largest of the areas; the smallest of the three areas with controls at 30° has, however, a double curvature with a general slope downward to the right, indicating that the reversing moment tends to increase with the angle of yaw until the airship finally becomes broadside to the wind.

The latter fact is more evident from the curves of righting moments due to the tails. With the exception of tails Nos. 1 and 3 at neutral, which reach a maximum value at 11° yaw, the general slope of these righting moment curves is upward to the right, while that due the 75% A_s begins to decline at 10° yaw even with the controls at 30°, indicating as said before, the inadequacy of this particular set of stabilizing surfaces.

Aspect Ratio Group.

The drag curves in this group of tail surfaces remain bunched together more than in any other group.

The lift curves have likewise the smallest variation, only at 15° yaw, with controls at 30°, tail No. 4 constitutes 150% of L_m, while with controls in neutral the contributions vary from 50 to 75% of L_m.

The reversing moments have the general shape, convex upward, with maximum values at large angles of yaw and of control setting.

The minimum values with controls in neutral position are very much like those for the area group, except the curve for tail No. 5 (the smallest aspect ratio) which almost coincides with the curve of reversing moments for the model alone.

From the curves of uprighting moments due to tails we observe that tail No. 4 (150% R_s) is the highest of the three curves, and No. 5 (75%) has the lowest, never rising more than one unit above the moment axis, while No. 4 for the same conditions gives a maximum effort of 4 lb.-in.

The explanation for the behavior of these tails is obviously due to the fact that the surface of least aspect ratio, being closest to the envelope is very inefficient, in the first place for performing in an airstream which is more or less turbulent, and secondly because of the well-known facts of aerodynamic effects on surfaces of reduced aspect ratio.*

The reverse is true about tail No. 4, its greater aspect ratio enabling it to extend more into the undisturbed airstream; furthermore, the center of pressure of these surfaces may travel in such a fashion as to favor tail No. 4 and disfavor tail No. 5.

Form Group.

Reference to the plots of performances for this group of stabilizing surfaces, including the standard, a rectangular form, and one with a balanced rudder indicates that the drags are practically the same as in the preceding two groups; 100% of D_m being offered

* Wilson, "Aeronautics," p. 16.

by the standard one at the greatest angles of yaw and control setting, and only 50% with the controls in neutral and 15° yaw.

From the lift point of view the rectangular surface (tail No. 8) is more efficient than either No. 1 or No. 6 (balanced).

All curves of lateral forces slope upward with the exception of No. 6 which declines when controls are in neutral.

The reversing moment on the airship is observed to be a minimum when fitted with tail No. 8 (rectangular) and in the vicinity of 12° yaw; the other two sets indicating a constantly increasing reversing moment when controls are in neutral position.

The curve of restoring moments for stabilizing surface No.8, is invariably higher than either No. 1 or No. 6, and with the exception of a single point (30° control and 15° yaw) at which the curve for standard form emerges from the rest the balanced rudder type of stabilizing surface is next best to the rectangular type.

Thickness Group.

The curves of longitudinal and transverse forces for this group of tail surfaces show that the drag is greatest for the thinnest section (No. 9), and least for the thickest one (No. 2), similarly the lateral force is greatest for the thinnest surface (No. 9), and least for the medium thickness (tail surface No. 7).

The reversing moment curves for tails Nos. 2 and 7 are very much alike and almost parallel, while the one for tail No. 9 is in all cases divergent and always above the other two.

Restoring moment curves for these stabilizing surfaces follow the same trend as those of reversing moments; the thickest section, No. 2, being very nearly a straight line. Curve No. 7 is slightly curved to the right, and No. 9, the thinnest tail surface, is approximately 50% more efficient than either of the other two.

The main conclusions of the experimental data plotted in Figs. 6, 7 and 8, for elevators at 10° may be summarized as follows:

(a) With the exception of the thinnest tail surface of the thickness group, and of the balanced rudder type of the form group, which run approximately 50% higher than the rest, for angles of pitch above 10°, all other tail units give drags varying from 12 to 25% that of the model alone at 0° angle of pitch, and from 50 to 100% that of the model alone at 15° angle of pitch; in the whole group the greatest drag variance being in the neighbothood of 25% the drag of the model alone.

(b) The thinnest section of the thickness group (having a surface 150% of standard area) gives 50% of the model lift over that of the standard tail surface; the least lift giving unit being the smallest of the area group, 75% A_S, as might have been expected, (See Fig. 7).

(c) The vital part of these experiments is clearly illustrated in Fig. 8, giving the righting moments of model with tail surface, and those due to the various tail units themselves. In these, the thinnest section (150%

A_{st}) is 25% better than that unit of the area group of the same surface.

The 50% standard thickness unit is slightly more efficient than that of the standard thickness of same area up to 10° pitch, but falls below the latter beyond that point.

Conclusions.

The curves of slope of righting moment (Figs. 13, 14 and 15) furnish a direct means of comparing the effectiveness of the various tail units. The form group having no rational basis of comparison, no attempt was made to represent these results graphically.

With the control surfaces in neutral, for example, these coefficients indicate greater effectiveness for larger areas and greater aspect ratios, but the curves drop somewhat for the 150% R_S when the control surfaces are set at 10°, presumably due to an excessive amount of turbulence generated by the elevators at high angles. With the exception of all 15° elevator curves which are more or less erratic, those for the area group are nearly straight line functions of the area, the aspect ratio ones have the same property for low elevator angles, and the thickness group indicates best effectiveness for the 50% T_S.

Figs. 16, 17, 18 and 19, representing collectively Figs. 6 to 8c inclusive, give lift, drag and moment curves for each group of tail surfaces for the same angle ($\beta = 10°$) of elevator setting.

BIBLIOGRAPHY OF PREVIOUS INVESTIGATIONS ON LIGHTER-THAN-AIR CRAFTS.

The most important investigations carried by different authorities, taken in chronological order, have been as follows:

1903 - "The Effects of Atmospheric Pressure on the Surfaces of Moving Envelopes." The results of these experiments were carried out by the Italians, Finzi and Soldati, in an attempt to discover the form of the solid of revolution which would offer the least resistance to motion and also to ascertain the effect of atmospheric pressure on various models; they were published in 1903.

1904 - "The Dynamics of Dirigibles" was originated by Col. Renard in 1904 who created the first theory of stability of airships.

1904 to 1907 - Col. Crocco seems to have been attributed the privilege of "bringing the airship to a stage of maturity." This he has accomplished in various publications of the "Bollettino della Societa Aeronautica Italiana," particularly those for April and June 1907.

1907 to date - Some work on the resistance of bodies of revolution has been done by M. Eiffel in his own laboratory and published in his early publications.

1910 to 1911 - The most exhaustive work on the subject, however, has been contributed by George Fuhrman of the Göttingen University in the famous "Theoretische und Experimentelle Untersuchungen an Ballon Modellen." In this investigation he carried his experiments on very thin, electrolitically deposited shells of various streamline forms. On these models the normal dynamic pressure on various points of the envelope was determined by means of fine perforations, one of them being open at a time. The integration of the horizontal components from the pressure distribution curve thus obtained enabled him to obtain the form resistance, which, when deducted from the total resistance measured by the balance, gave him the surface friction of the model.

Other books and publications I have freely consulted are:

(1) British Advisory Committee for Aeronautics Reports and Memoranda, Nos. 361, 102, 307 and 623.

(2) National Advisory Committee for Aeronautics Reports: No. 133 - "The Tail Plane," by Max M. Munk; No. 136 - "Damping Coefficient due to Tail Surfaces," Chu-Warner; No. 138 - "The Drag of "C" Class Airships," Zahm, Smith-Hill.

(3) N.A.C.A. Technical Notes Nos. 104, 105 and 106, on Aerodynamic Forces, by Munk. N.A.C.A. Technical Note No. 63, by Nobile on Limits of Useful Load of Airships.

(4) Hunsaker: "Wind Tunnel Experiments" and "Dynamical Stability." Smithsonian Miscellaneous Collection, Vol. 62, No. 4.

(5) Bryan: "Stability in Aviation."

(6) Wislon: "Aeronautics."

(7) Lamb: "Hydrodynamics."

(8) Brauzzi: "Cours d'Aeronautique Generale."

(9) Bairstow: "Applied Aerodynamics."

(10) Bianchi: "Dinamica del Dirigible."

(11) U.S.N. Aeronautical Reports (Construction and Repair) Nos. 194, 150 and 161.

(12) "La Technique Aeronautique," June, 1911.

(13) "Motorluftschiff-Studiengesellschaft," Fünfter Band, 1911-1912.

(14) "Maximum Limit of Useful Load of Airships," by Col. Crocco ("Rendiconti dell' Istituto Sperimentalle Aeronautico," Roma, September, 1920).

Data on Model Alone.

Airspeed 40 M.P.H.

TABLE III.

Angle of Yaw	Measured Forces in Grams			
	0^o	5^o	10^o	15^o
Drag D_1	73	82	59	78
Drag D_2	143	153	142	183
Model Drag	70	71	83	105
Balance Drag	19	18	17	16
Correct D_m	51	53	66	89
Front R_1	97	76	57	45
Front R_2	94	136	200	225
Front $Lift_1$	-3	60	143	180
Rear R_1	95	60	132	86
Rear R_2	105	14	80	50
Rear $Lift_2$	10	-46	-53	-36
Total Lift	7	14	91	144
Moment (g-cm)	-465	+4385	+8418	+9823

Moments are taken about center of buoyancy assumed coincident with the center of volume, and determined by the expression:

$$M = D'z + R'x - R'y$$

where $x = 1.348 \cos \alpha$.

$y = 1.159 \cos \alpha$

and $z = 2.000 \sin \alpha$

(See Fig. 4)

L. Elevators in Neutral Position

Table of Longitudinal Forces (grams)

TABLE IV.

Angle of yaw	Model alone	Forces on Area Group			Aspect Ratio Group		
		As	150%	75%	Rs	75%	150%
0	52	54	50	51	54	55	54
5	54	50	59	53	50	54	60
10	67	72	71	77	72	75	81
15	91	115	131	118	115	125	117
		Lateral Forces in Grams					
0	7	0	0	0	0	8	0
5	14	63	58	27	63	26	49
10	91	130	157	127	130	114	155
15	144	248	296	224	248	217	268
		Table of Moments about C.B. (lb.in.)					
0	-.41	0.00	0.00	0.00	0.00	0.34	0.00
5	3.78	2.51	1.80	3.12	2.51	3.28	2.68
10	7.28	4.80	3.40	5.29	4.80	7.38	4.35
15	8.48	6.76	3.25	6.92	6.76	7.33	4.41
		Table of Moments Due to Tails (lb.in.)					
0	00.41	00.41	00.41	00.41	00.41	00.75	00.41
5		-1.27	-1.98	-0.66	-1.27	- .50	-1.10
10		-2.48	-3.88	-1.99	-2.48	- .10	-2.93
15		-1.72	-5.23	-1.56	-1.72	-1.15	-4.07

Elevators in Neutral Position

Table of Longitudinal Forces (grams)

TABLE IV (Cont.)

Angle of yaw	Model alone	Form Group			Thickness Group		
		Fs	Rud-der Bal.	Rectan-gular	Ts	50%	12%
0	52	54	53	57	54	58	58
5	54	50	62	57	50	61	68
10	67	72	76	77	72	85	95
15	91	115	118	112	115	118	157
		Lateral Forces in Grams					
0	7	0	11	-4	0	21	-5
5	14	63	63	30	58	37	67
10	91	130	126	132	157	142	178
15	144	248	158	280	296	313	322
		Table of Moments about C.B. (lb.in.)					
0	-.41	0.00	0.13	-.12	0.00	2.14	-.18
5	3.78	2.51	1.80	2.46	1.80	2.99	1.64
10	7.28	4.80	4.35	4.69	3.40	4.16	1.17
15	8.48	6.76	7.56	4.33	3.25	3.73	1.28
		Table of Moments Due to Tails (lb.in.)					
0	00.41	00.41	00.54	00.29	00.41	2.55	00.23
5		-1.27	-1.98	-1.32	-1.98	-.79	-2.14
10		-2.48	-2.93	-2.59	-3.88	-3.12	-6.11
15		-1.72	- .92	-4.15	-5.23	-4.75	-7.20

Elevators Set at 10°

Table of Longitudinal Forces (grams)

TABLE V.

Angle of yaw	Model alone	Forces on Area Group			Aspect Ratio Group		
		As	150%	75%	Rs	75%	150%
0	52	57	67	54	57	54	59
5	54	66	75	63	66	66	68
10	67	91	101	85	91	93	93
15	91	155	168	140	155	126	141
Table of Lateral Forces (grams)							
0	7	30	48	35	30	32	58
5	14	59	91	75	59	78	93
10	91	137	205	127	137	159	180
15	144	323	359	248	323	265	318
Table of Moments about C.B. (lb.in.)							
0	-.41	-.92	-1.47	0.54	-.92	-1.03	-1.11
5	3.78	1.27	0.13	2.34	1.27	1.48	0.85
10	7.28	2.89	0.80	3.92	2.89	3.11	1.81
15	8.48	1.88	-1.09	4.76	1.88	3.94	- .19
Table of Moments Due to Tails (lb.in.)							
0		- .51	-1.06	-0.95	- .51	- .62	- .70
5		-2.51	-3.65	-1.44	-2.51	-2.30	-2.93
10		-4.39	-6.48	-3.36	-4.39	-4.17	-5.47
15		-6.60	-9.57	-3.72	-6.60	-4.54	-8.67

Elevators Set at 10°

Table of Longitudinal Forces (grams)

TABLE V (Cont.)

Angle of yaw	Model alone	Form Group			Thickness Group		
		Fs	Rudder Bal.	Rectan-gular	Ts	50%	12%
0	52	57	60	63	67	62	65
5	54	66	65	73	75	73	74
10	67	91	91	99	101	96	114
15	91	155	208	142	168	150	188
		Table of Lateral Forces (grams)					
0	7	30	31	45	48	34	39
5	14	59	64	107	91	102	115
10	91	137	164	185	205	202	255
15	144	323	323	383	359	344	418
		Table of Moments about C.B. (lb.in.)					
0	-.41	-.92	-1.61	-1.85	-1.47	-2.00	-2.62
5	3.78	1.27	0.33	- .08	0.13	- .08	-1.06
10	7.28	2.89	1.83	1.66	0.80	0.66	-1.74
15	8.48	1.88	2.72	0.51	-1.09	0.59	-3.07
		Table of Moments Due to Tails (lb.in.)					
0	- .51	- .51	-1.20	-1.44	-1.06	-1.59	-2.21
5	-2.51	-2.51	-3.45	-3.86	-3.65	-3.86	-4.84
10	-4.39	-4.39	-5.45	-5.62	-6.48	-6.62	-9.02
15	-6.60	-6.60	-5.76	-7.92	-9.57	-7.89	-11.55

Elevators Set at 20°

Table of Longitudinal Forces (grams)

TABLE VI.

Angle of yaw	Model alone	Forces on Area Group			Aspect Ratio Group		
		As	150%	75%	Rs	75%	150%
0	52	58	73	58	58	59	66
5	54	69	87	59	69	72	78
10	67	96	120	91	96	105	109
15	91	147	204	129	147	147	157
Table of Lateral Forces (grams)							
0	7	56	105	45	56	68	70
5	14	101	162	103	101	90	129
10	91	170	248	164	170	170	222
15	144	338	390	274	338	327	387
Table of Moments about C.B. (lb.in.)							
0	-.41	-1.72	-4.20	-1.58	-1.72	-2.76	-3.73
5	3.78	- .34	-3.17	1.28	- .34	0.03	- .95
10	7.28	1.62	-2.13	2.86	1.62	1.44	- .20
15	8.48	1.98	-3.04	3.06	1.98	2.07	- .85
Table of Moments Due to Tails (lb.in.)							
0		-1.31	-3.79	-1.17	-1.31	-2.35	-3.32
5		-4.12	-6.95	-2.50	-4.12	-3.75	-4.73
10		-5.66	-9.41	-4.42	-5.66	-5.84	-7.48
15		-6.50	-11.52	-5.42	-6.50	-6.41	-9.33

Elevators Set at 20°

Table of Longitudinal Forces (grams)

TABLE VI (Cont.)

Angle of yaw	Model alone	Form Group			Thickness Group		
		Fs	Rudder Bal.	Rectan-gular	Ts	50%	12%
0	52	58	67	65	73	66	71
5	54	69	77	79	87	84	91
10	67	96	112	108	120	115	136
15	91	147	166	156	204	177	221
		Table of Lateral Forces (grams)					
0	7	56	29	83	105	78	110
5	14	101	99	143	162	124	182
10	91	170	207	233	248	261	309
15	144	338	334	370	390	404	514
		Table of Moments about C.B. (lb.in.)					
0	-.41	-1.72	-4.66	-3.81	-4.20	-3.66	-5.15
5	3.78	- .34	-2.01	-1.91	-3.17	-2.55	-4.68
10	7.28	1.62	0.14	-0.76	-2.13	-1.98	-5.01
15	8.48	1.98	0.51	-0.51	-3.04	-1.61	-7.24
		Table of Moments Due to Tails (lb.in.)					
0		-1.31	-4.25	-3.40	-3.79	-3.25	-4.74
5		-4.12	-5.79	-5.69	-6.95	-6.33	-8.46
10		-5.66	-7.14	-8.04	-9.41	-9.26	-12.29
15		-6.50	-7.97	-8.99	-11.52	-10.09	-15.72

Elevators Set at 30°

Table of Longitudinal Forces (grams)

TABLE VII.

Angle of yaw	Model alone	Forces on Area Group			Aspect Ratio Group		
		As	150%	75%	Rs	75%	150%
0	52	67	84	56	67	74	77
5	54	91	102	73	91	86	93
10	67	129	141	100	129	122	130
15	91	194	220	148	194	177	183
		Table of Lateral Forces (grams)					
0	7	106	77	71	106	63	61
5	14	157	178	103	157	137	169
10	91	227	288	172	227	220	274
15	144	373	438	284	373	374	403
		Table of Moments about C.B. (lb.in.)					
0	-0.41	-3.75	-5.74	-1.19	-3.75	-3.92	-3.84
5	3.78	-2.29	-4.66	- .67	-2.29	-1.49	-3.60
10	7.28	-2.03	-4.36	1.68	-2.03	0.29	-2.37
15	8.48	-3.39	-5.63	2.91	-3.39	1.02	-3.47
		Table of Moments due to Tails (lb.in.)					
0		-3.34	-5.33	-0.78	-3.34	-3.51	-3.43
5		-6.07	-8.44	-4.45	-6.07	-5.27	-7.38
10		-9.31	-11.64	-5.60	-9.31	-6.99	-9.65
15		-11.87	-14.11	-5.57	-11.87	-7.46	-11.95

Elevators Set at 30°

Table of Longitudinal Forces (grams)

TABLE VII (Cont.)

Angle of yaw	Model alone	Form Group			Thickness Group		
		Fs	Rudder Bal.	Rectan-gular	Ts	50%	12%
0	52	67	73	76	84	86	80
5	54	91	91	88	102	111	108
10	67	129	120	119	141	158	164
15	91	194	187	175	220	223	262

Table of Lateral Forces (grams)

0	7	106	84	109	77	124	119
5	14	157	146	178	178	202	232
10	91	227	237	247	288	316	377
15	144	373	365	369	438	484	540

Table of Moments about C.B. (lb.in.)

0	-0.41	-3.75	-4.29	-4.87	-5.74	-6.45	-2.72
5	3.78	-2.29	-2.72	-2.59	-4.66	-5.93	-6.90
10	7.28	-2.03	- .63	-2.12	-4.36	-5.79	-7.53
15	8.48	-3.39	-1.51	-2.12	-5.63	-6.28	-9.60

Table of Moments Due to Tails (lb.in.)

0		-3.34	-3.88	-4.46	-5.33	-6.04	-2.31
5		-6.07	-6.50	-6.35	-8.44	-9.71	-10.68
10		-9.31	-7.91	-9.40	-11.64	-13.07	-14.81
15		-11.87	-9.99	-10.60	-14.11	-14.76	-18.08

Slope of Righting Moment Curves

Stabilizers in Neutral

TABLE VIII.

Tail Unit	0° Yaw	5° Yaw	10° Yaw	15° Yaw	Group	Remarks
Stand. A_S	-.42	-.40	-.36	-.27		Min. at 12.5°
150%	-.32	-.30	-.20	+.15	Area	No minimum
75%	-.55	-.45	-.33	-.10		No minimum
Stand. R_S	-.41	-.41	-.36	-.32		Min. at 12.5°
150%	-.33	-.65	-.33	+.31	Asp. Rat.	No minimum
75%	-.46	-.36	-.16	+.10		Min. at 12.5°
Rectang.	-.43	-.41	-.35	-.31		No minimum
Bal. Rud.	-.23	-.37	-.48	-.55	Form	No minimum
F_S	-.38	-.49	-.16	+.31		Min. at 12°
T_S No.1	-.37	-.33	-.12	+.23		Min. at 12.5°
50% No.2	-.18	-.22	-.10	+.26	Thickness	Min. at 11.4°
12½% No.3	-.37	-.11	+.13	-.20		Max. at 11.5°

Slope of Righting Moment Curves

Stabilizer at 10°

TABLE IX.

Tail Unit	0° Yaw	5° Yaw	10° Yaw	15° Yaw	Group	Remarks
150% A_S	-.29	-.22	0	+.57		0 at 9°+
A_S	-.38	-.37	-.12	+.35	Area	0 at 11°
75% A_S	-.32	-.30	-.22	-.03		No minimum
R_S	-.39	-.25	0	-.66		0 at 10.5°
150%	-.42	-.36	-.09	+.37	Asp. Rat.	0 at 11°
75%	-.42	-.36	-.20	0		0 at 15°
Rectang.	-.33	-.28	-.12	+.48		Min. at 11°
Bal. Rud.	-.35	-.28	-.21	-.05	Form	No minimum
F_S	-.38	-.33	-.11	+.47		Min. at 11.5°
T_S	-.48	-.04	+.20	+.25		Min. at 5.5°
50%	-.44	-.25	+.08	+.48	Thickness	Min. at 9°+
12½%	-.31	-.20	-.03	+.09		Min. at 12°

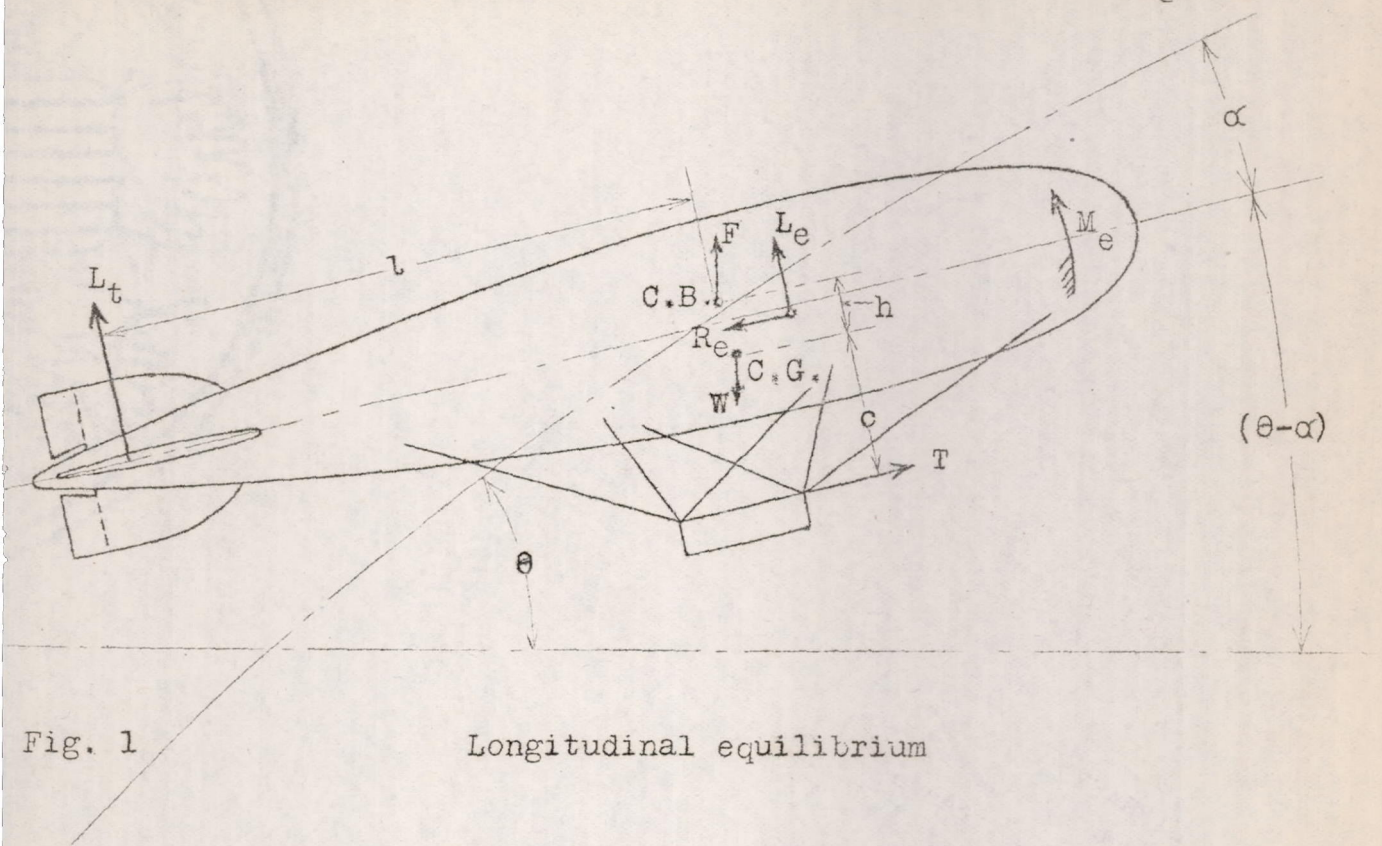

Fig. 1 Longitudinal equilibrium

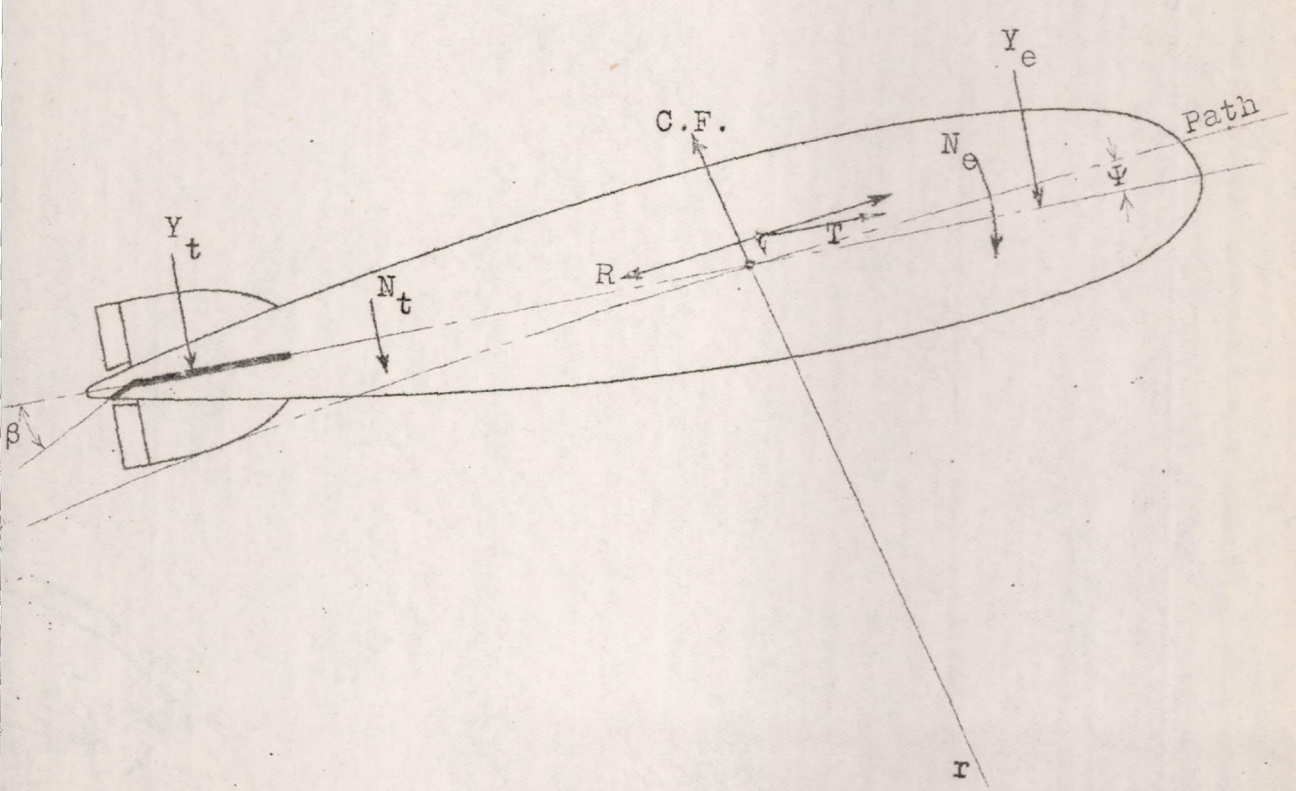

Fig. 2 Directional equilibrium

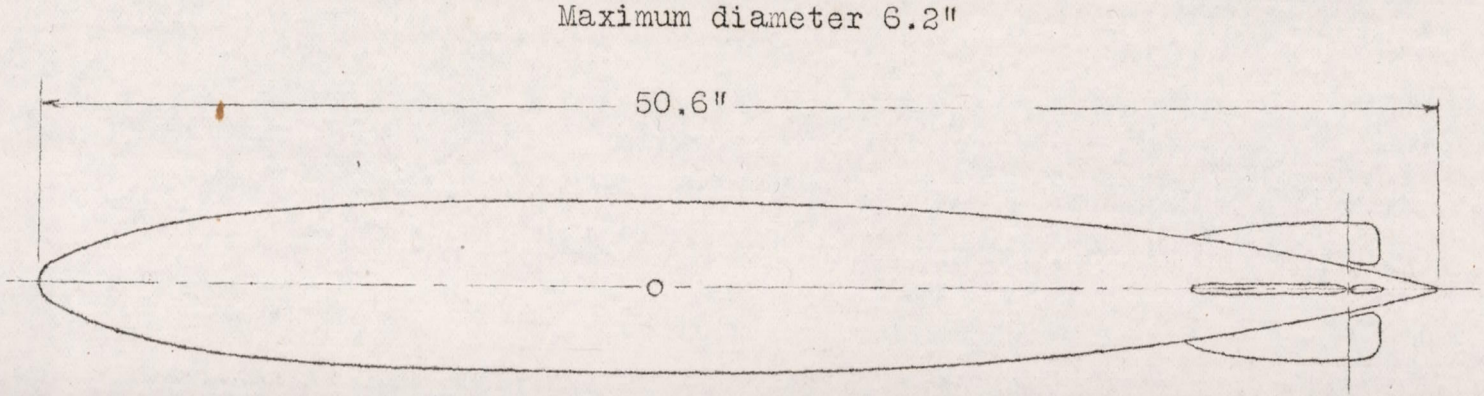

Scale of model 1/153
full size

Model standard tail surfaces				
Horizontal fins	= 13.16	sq.in.	(84.90	cm^2)
Vertical "	= 13.16	" "	(84.90	")
Horizontal controls	= 3.80	" "	(24.52	")
Vertical "	= 3.80	" "	(24.52	")

Fig. 3 Experiments on the Zeppelin L-33

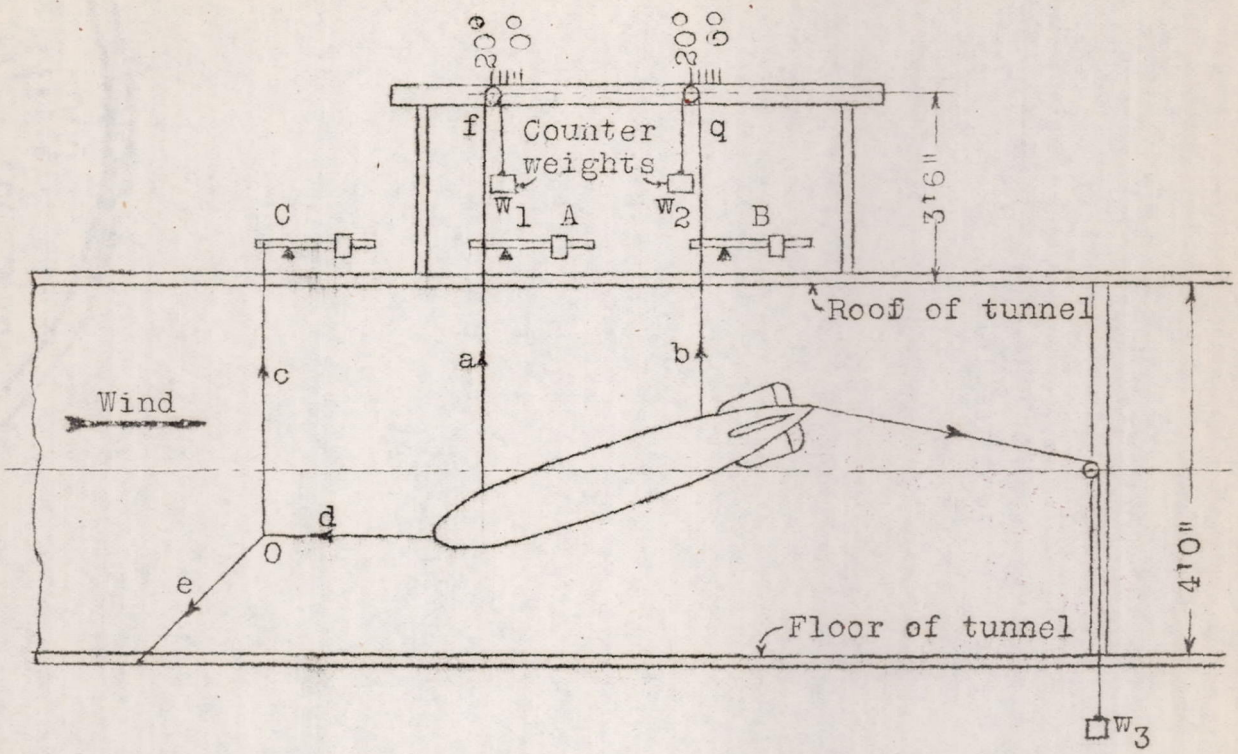

Fig. 4 General arrangement of apparatus

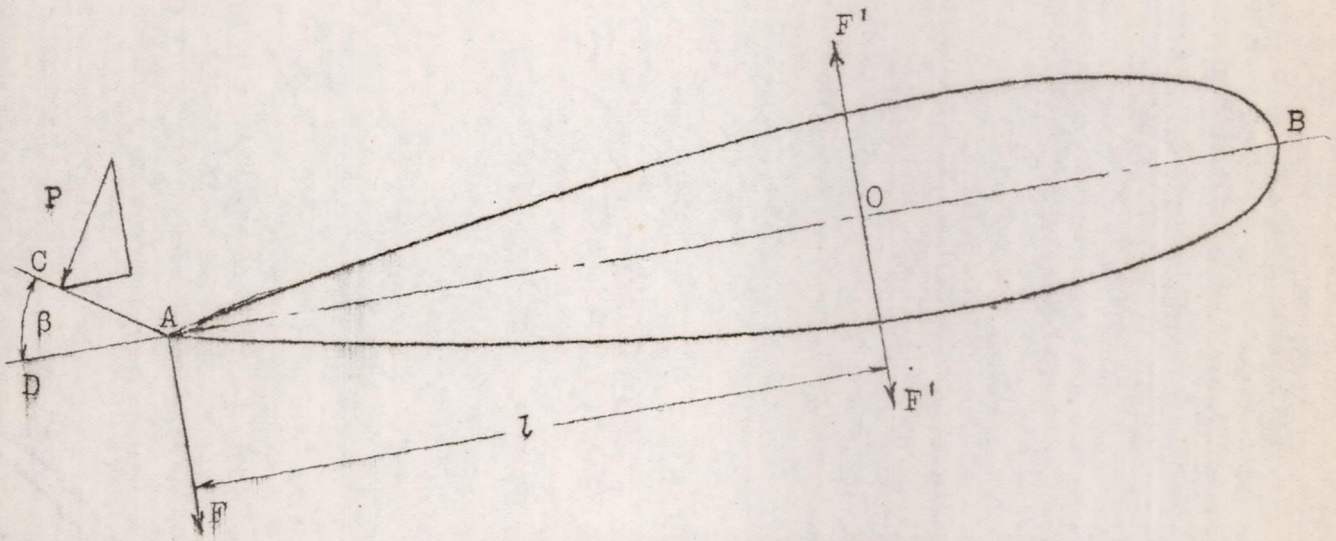

Fig. 5 Force diagram

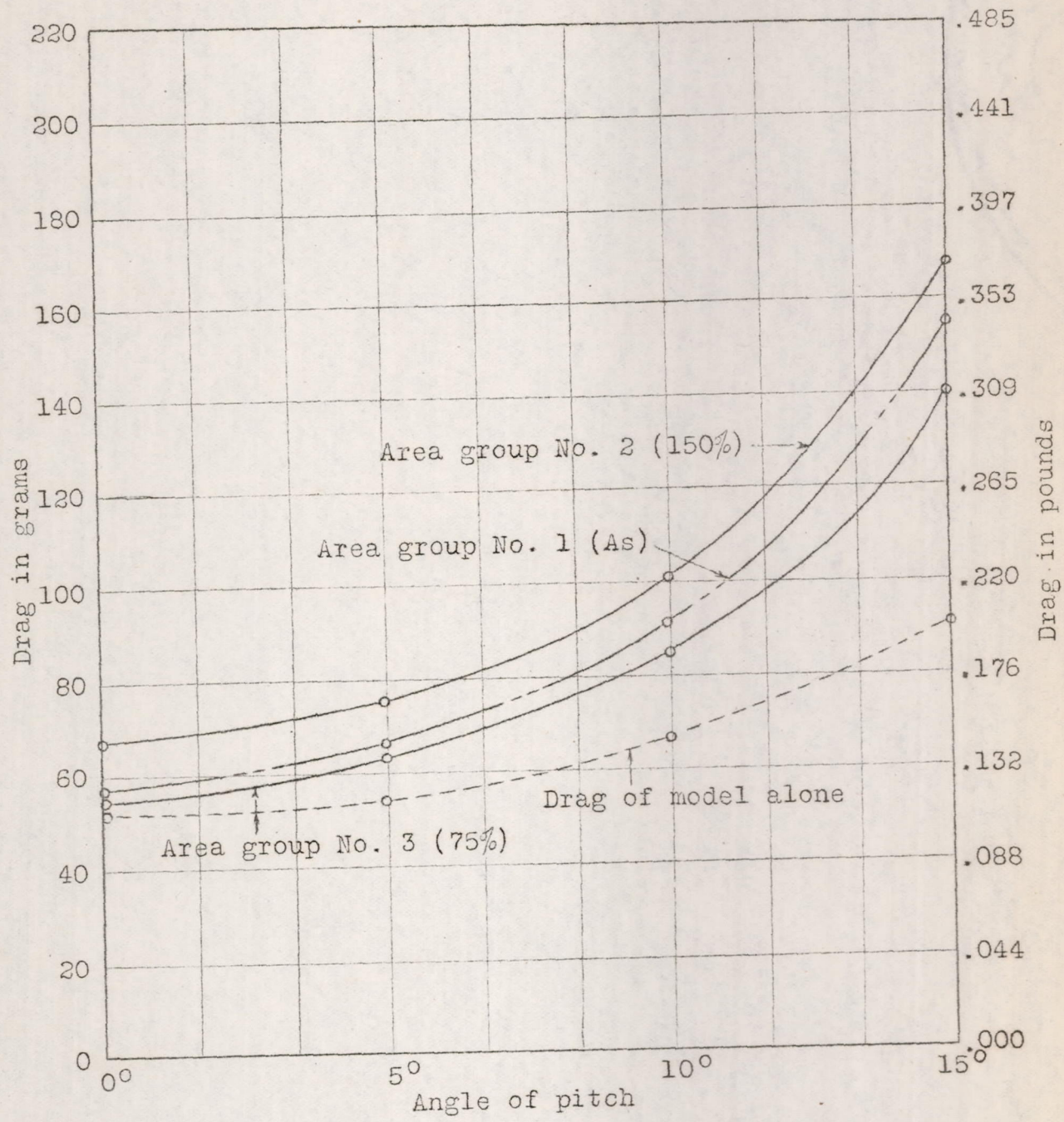

Fig. 6 Drag curves for elevator angle 10°

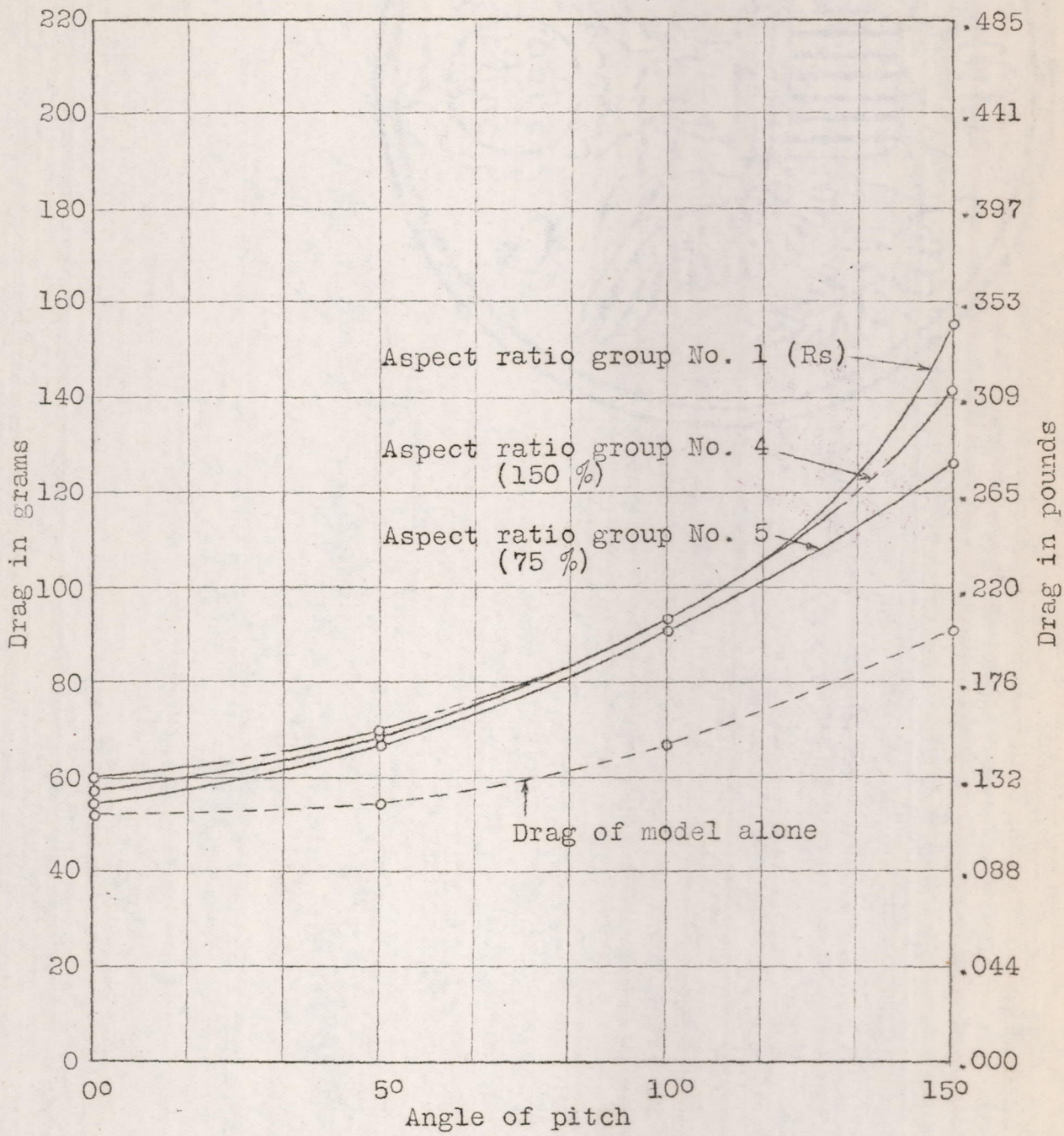

Fig. 6a Drag curves for elevator angle 10°

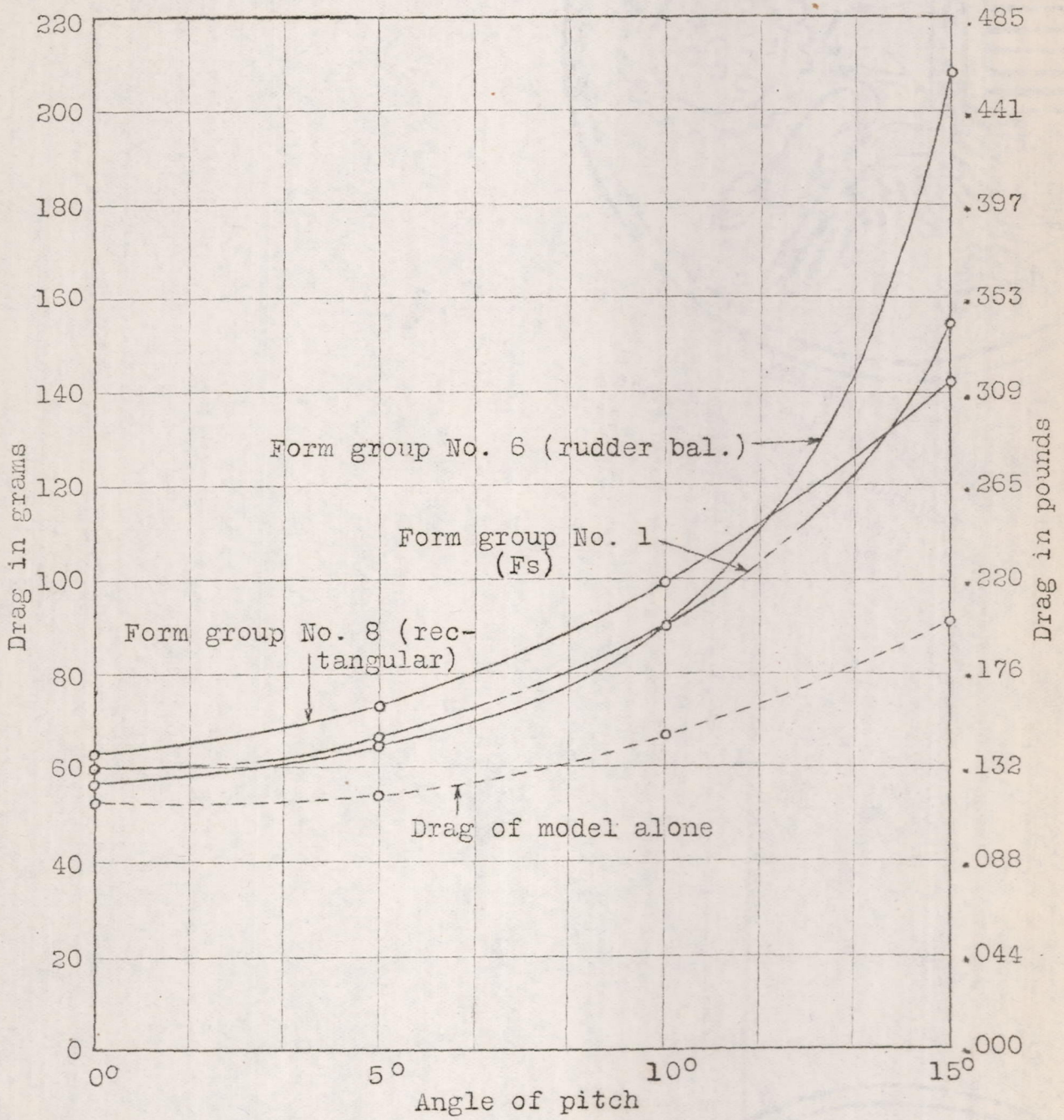

Fig. 6b Drag curves for elevator angle 10°

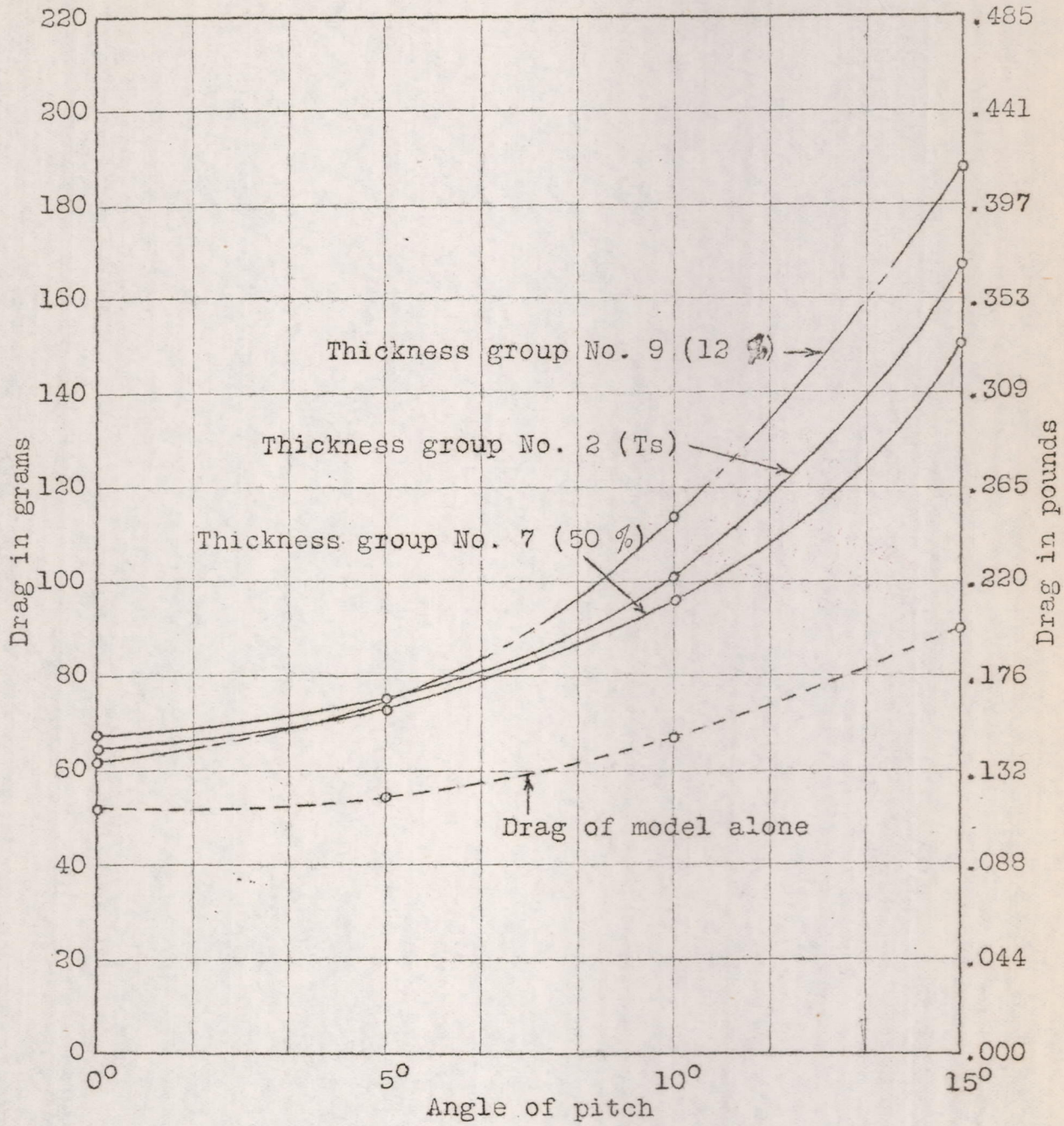

Fig. 6c Drag curves for elevator angle 10°

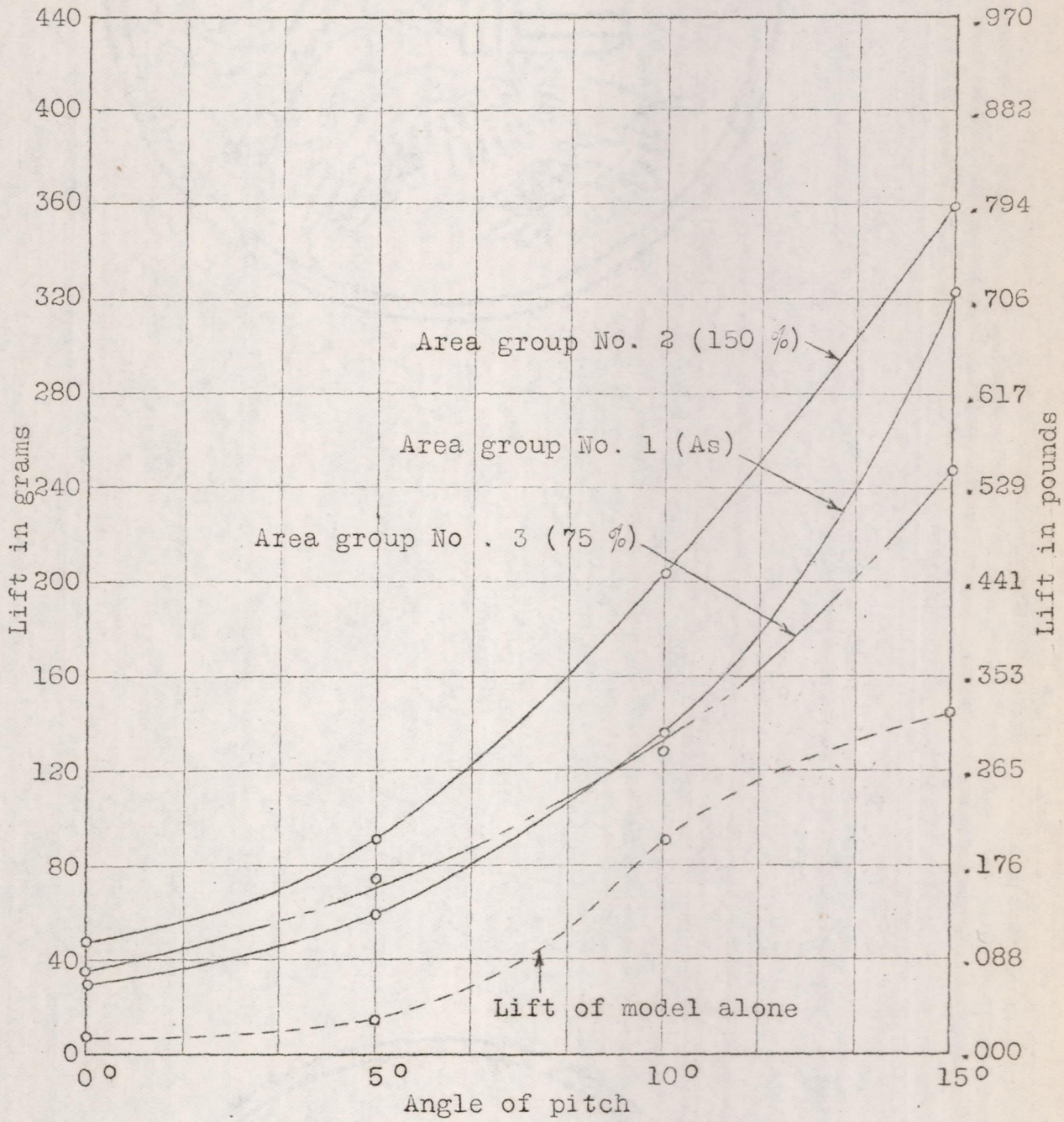

Fig. 7 Lift curves for elevator angle 10°

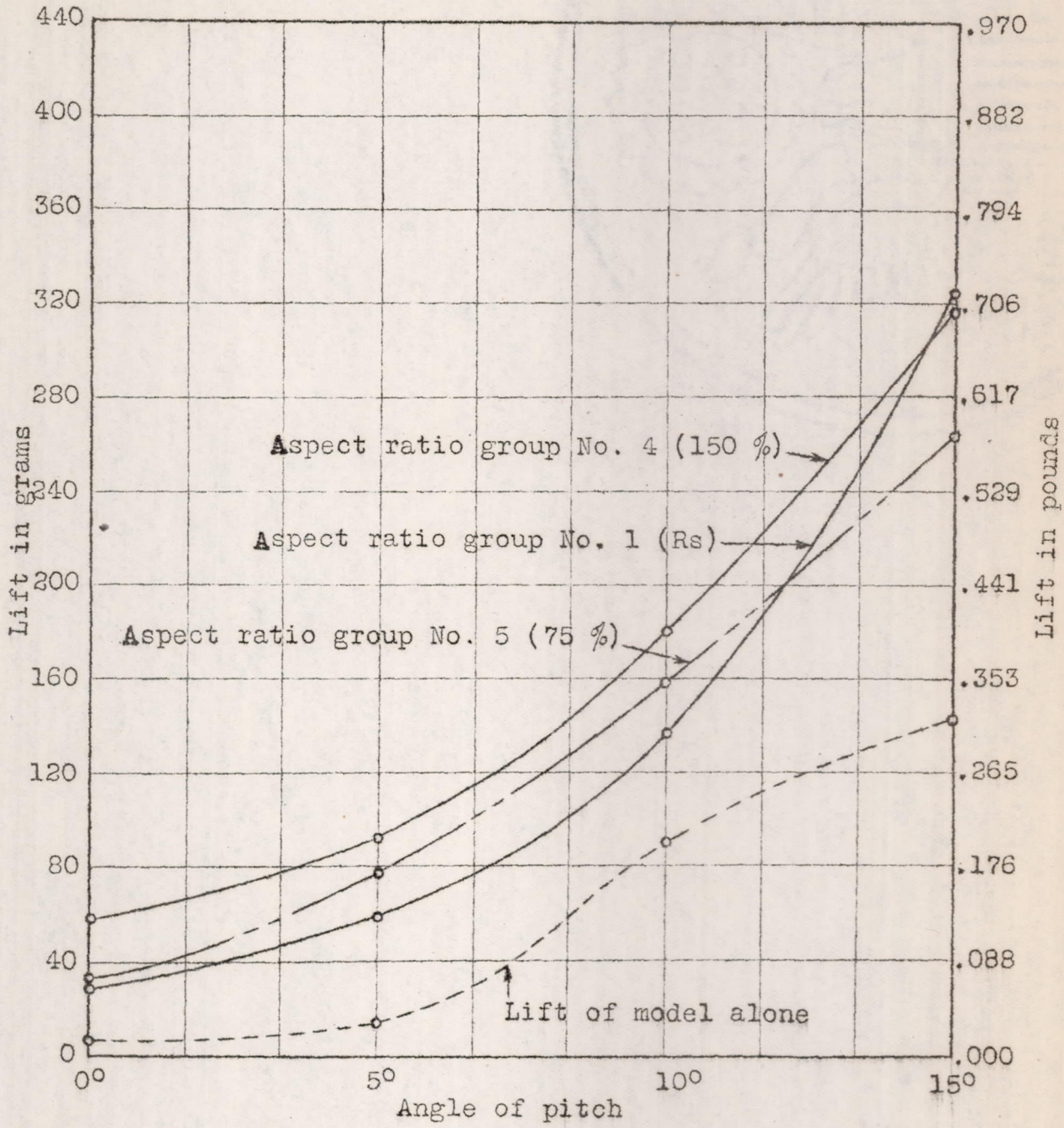

Fig. 7a Lift curves for elevator angle 10°

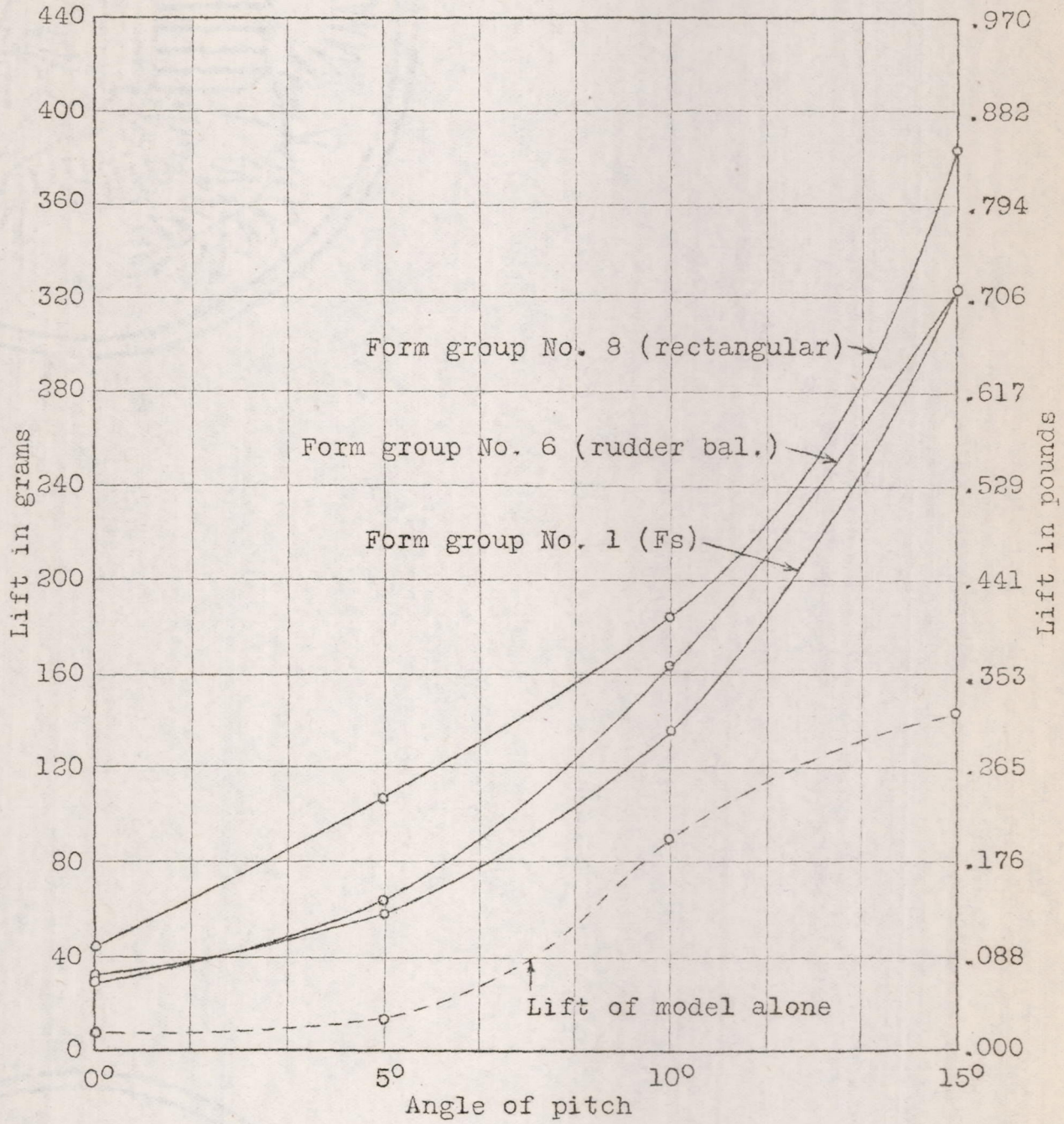

Fig. 7b Lift curves for elevator angle 10°

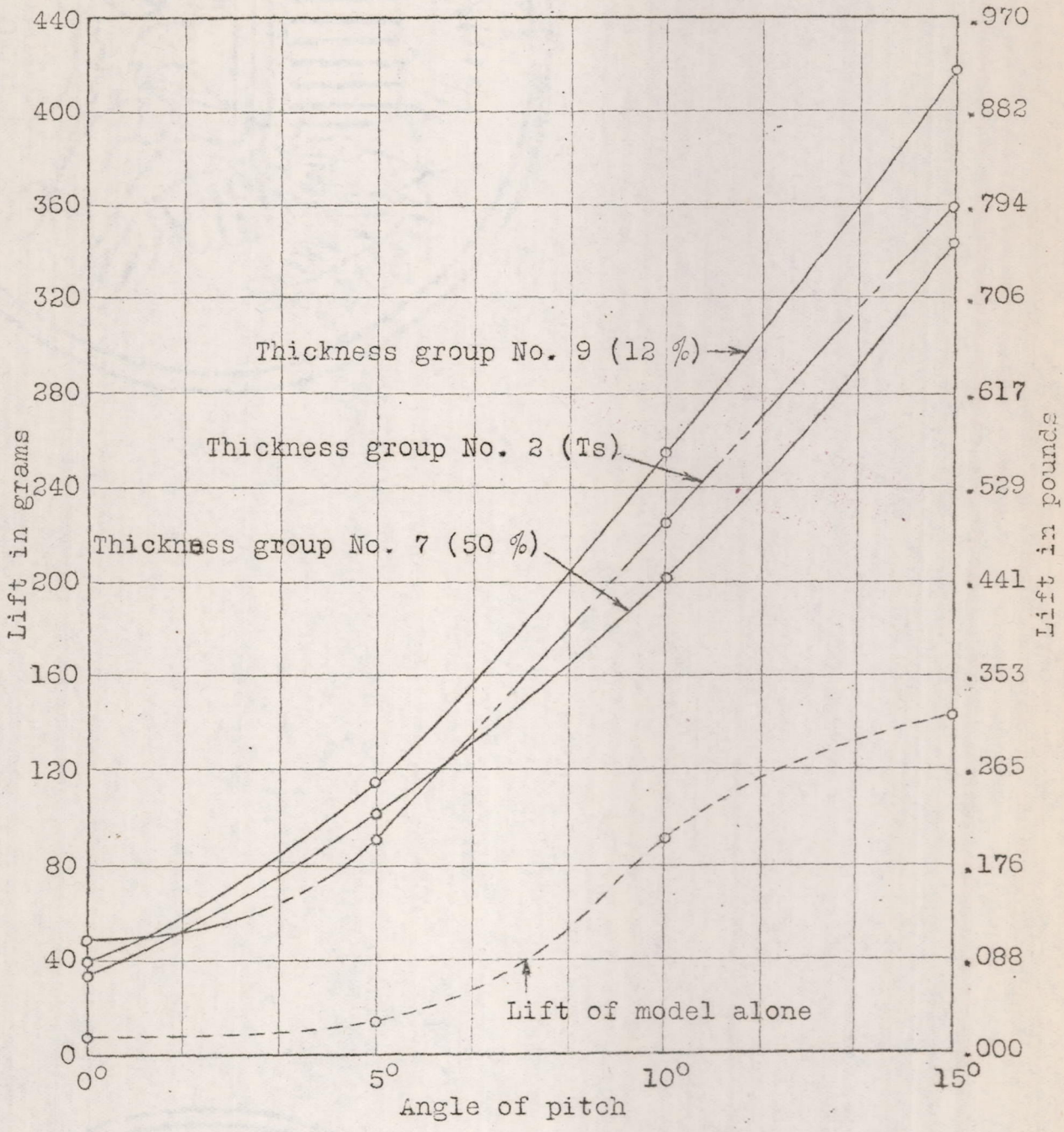

Fig. 7c Lift curves for elevator angle 10°

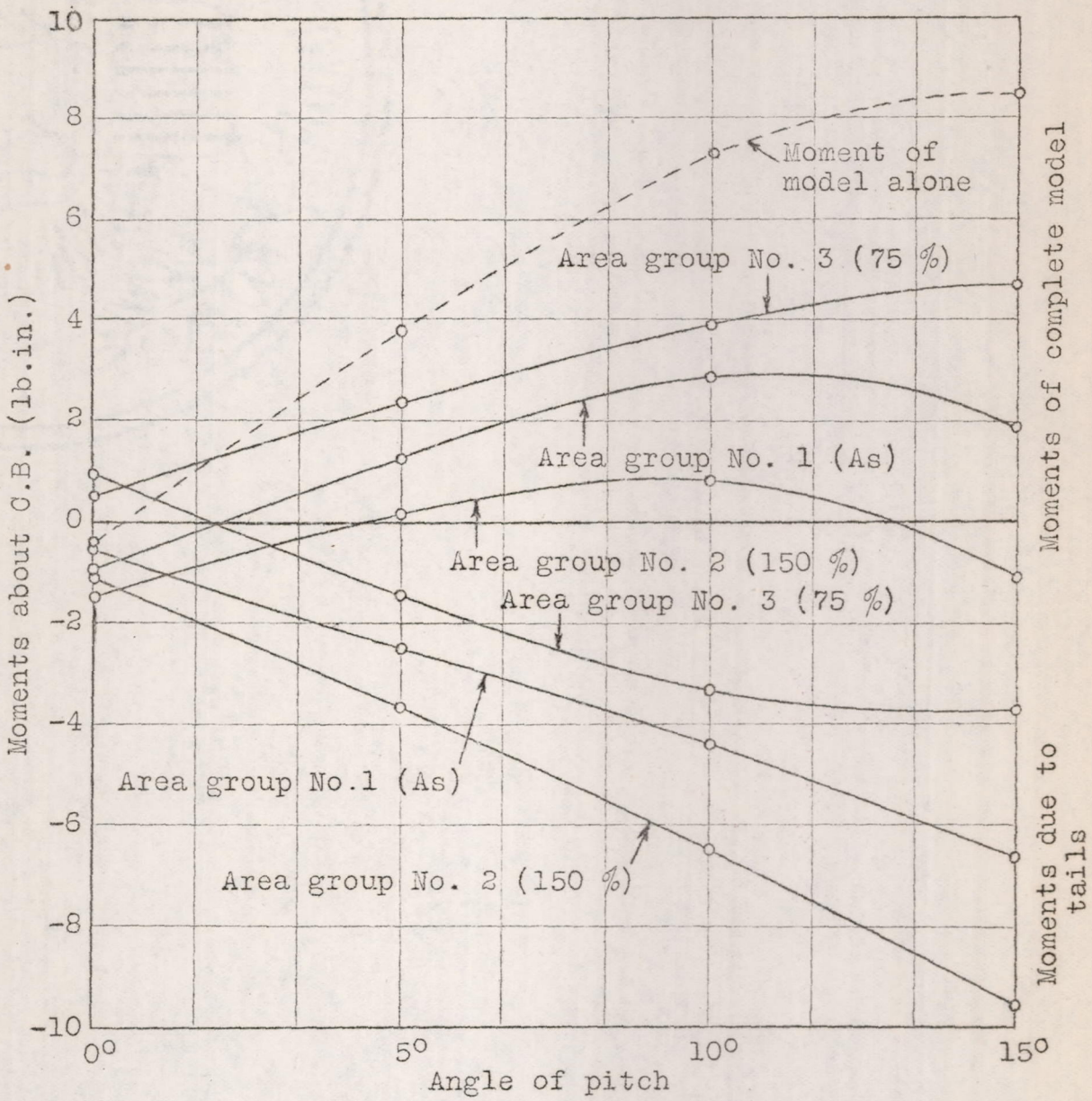

Fig. 8 Moment curves for elevator angle 10°

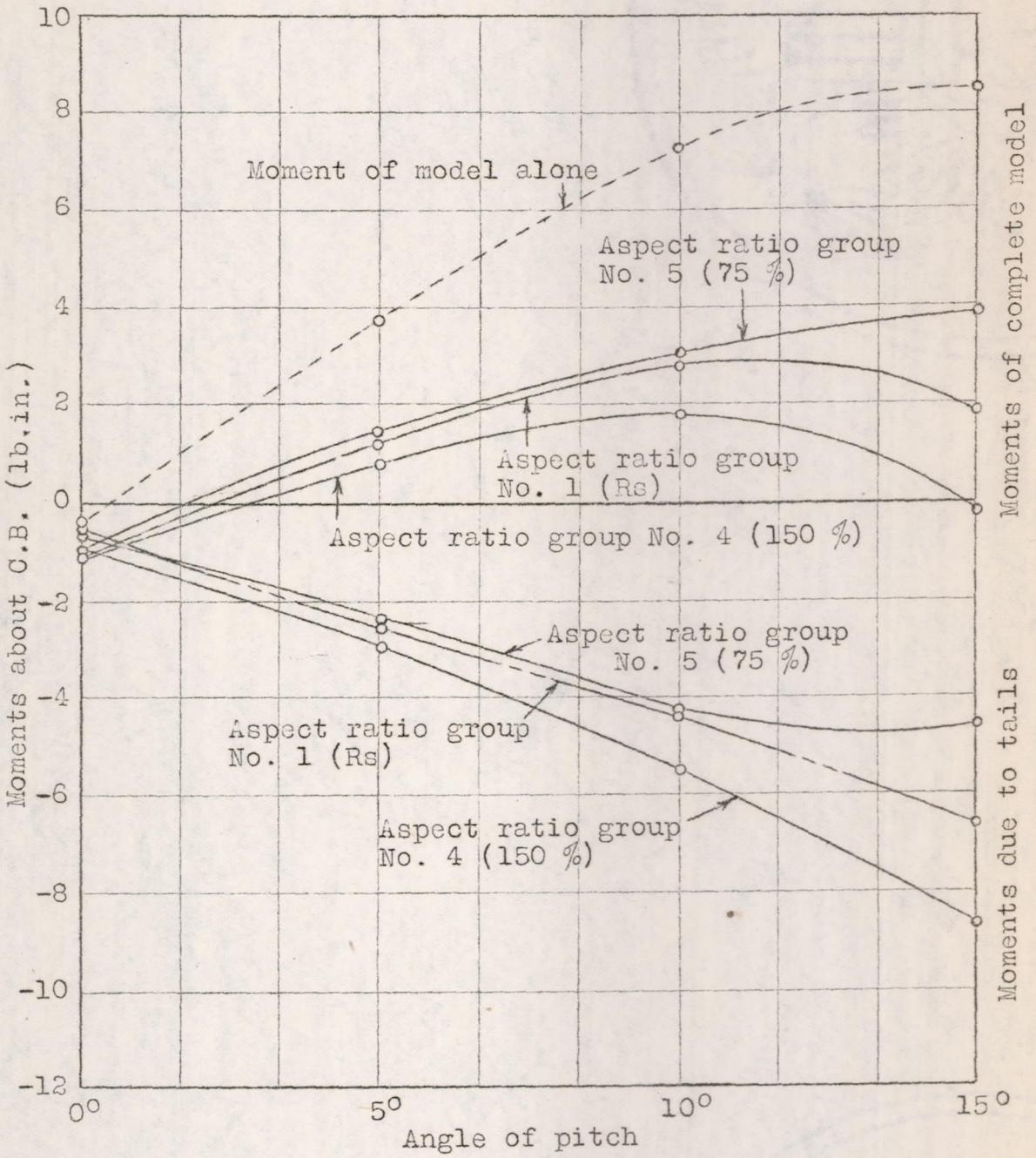

Fig. 8a Moment curves for elevator angle 10°

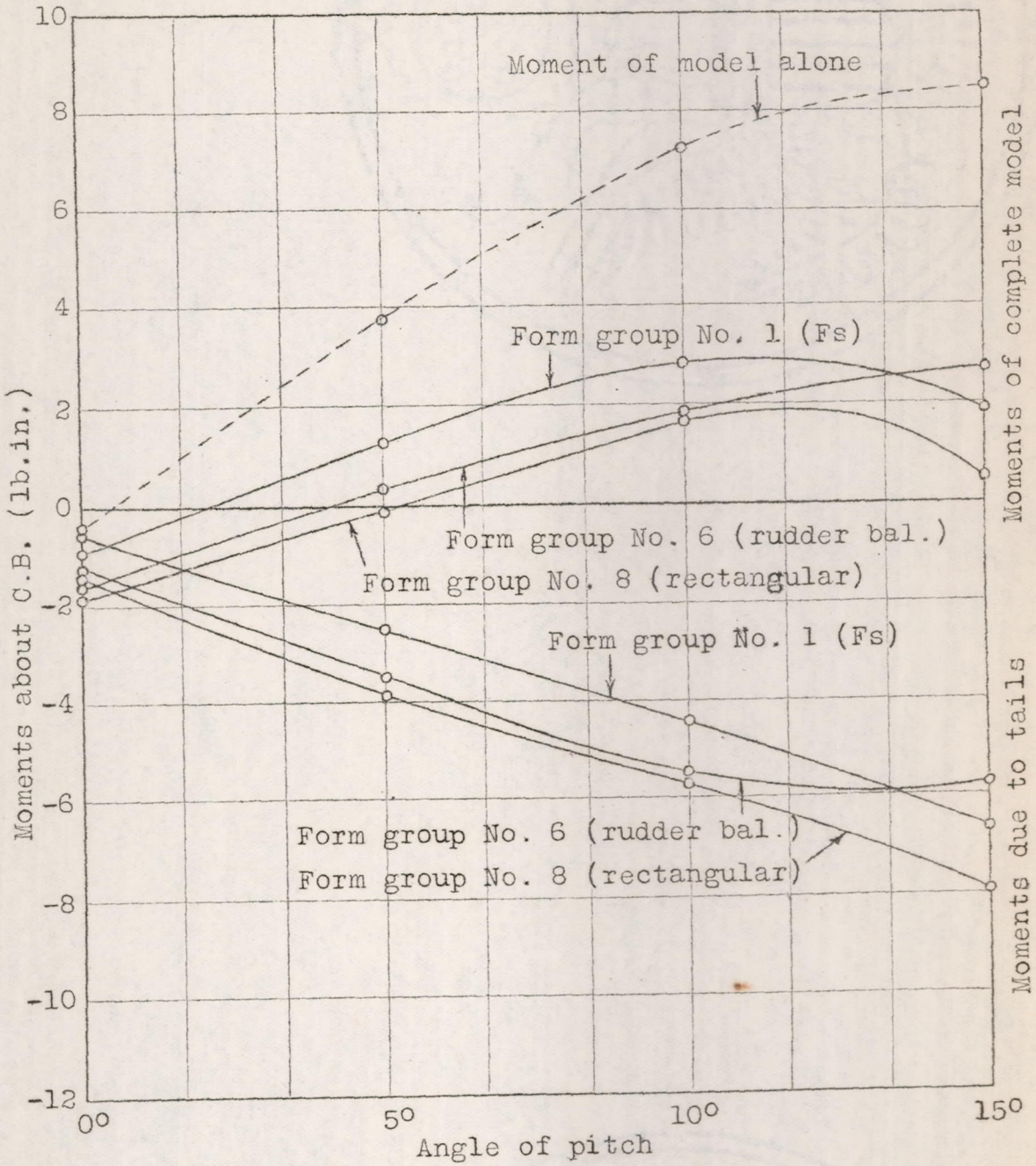

Fig. 8b Moment curves for elevator angle 10°

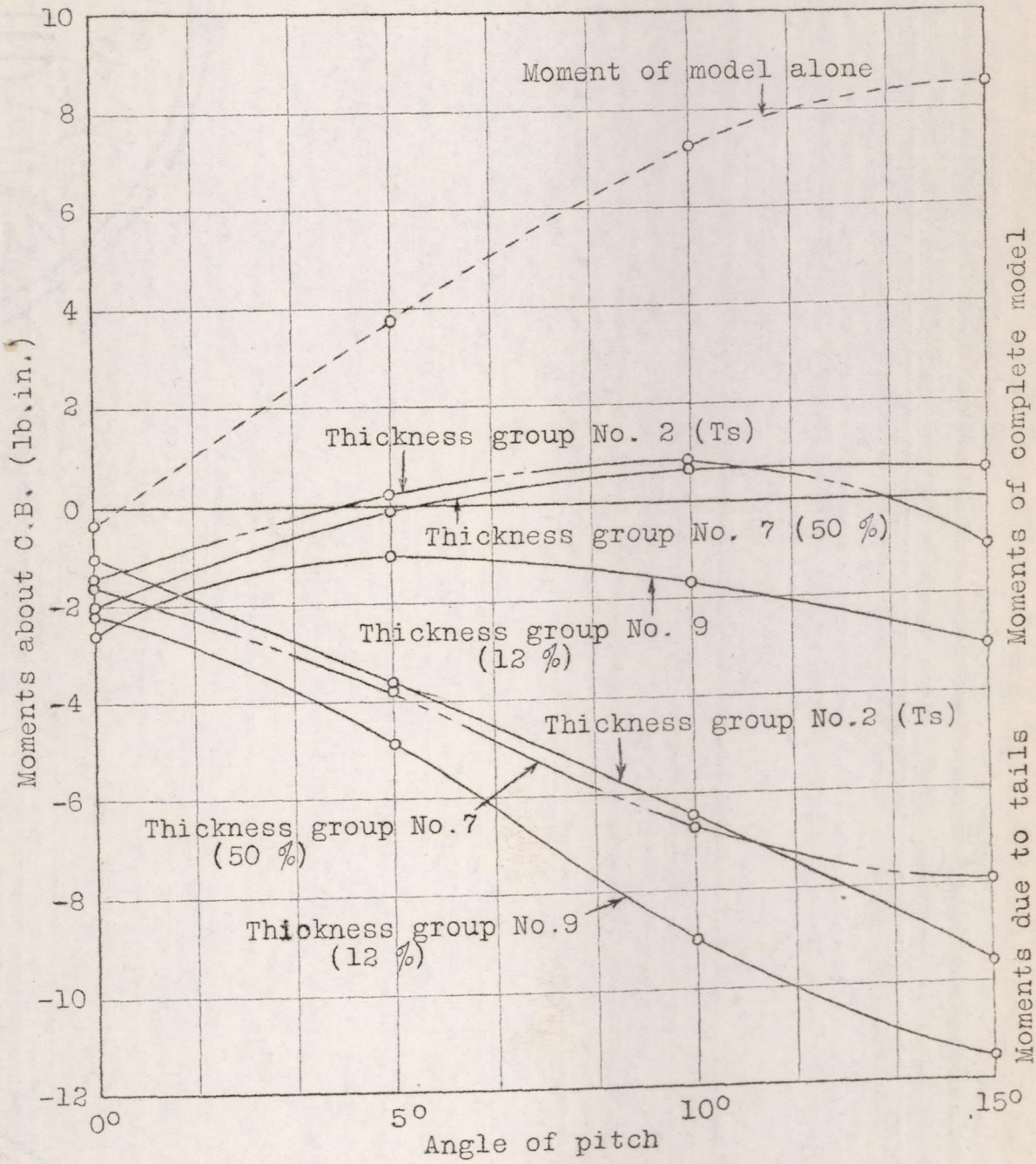

Fig. 8c Moment curves for elevator angle 10°

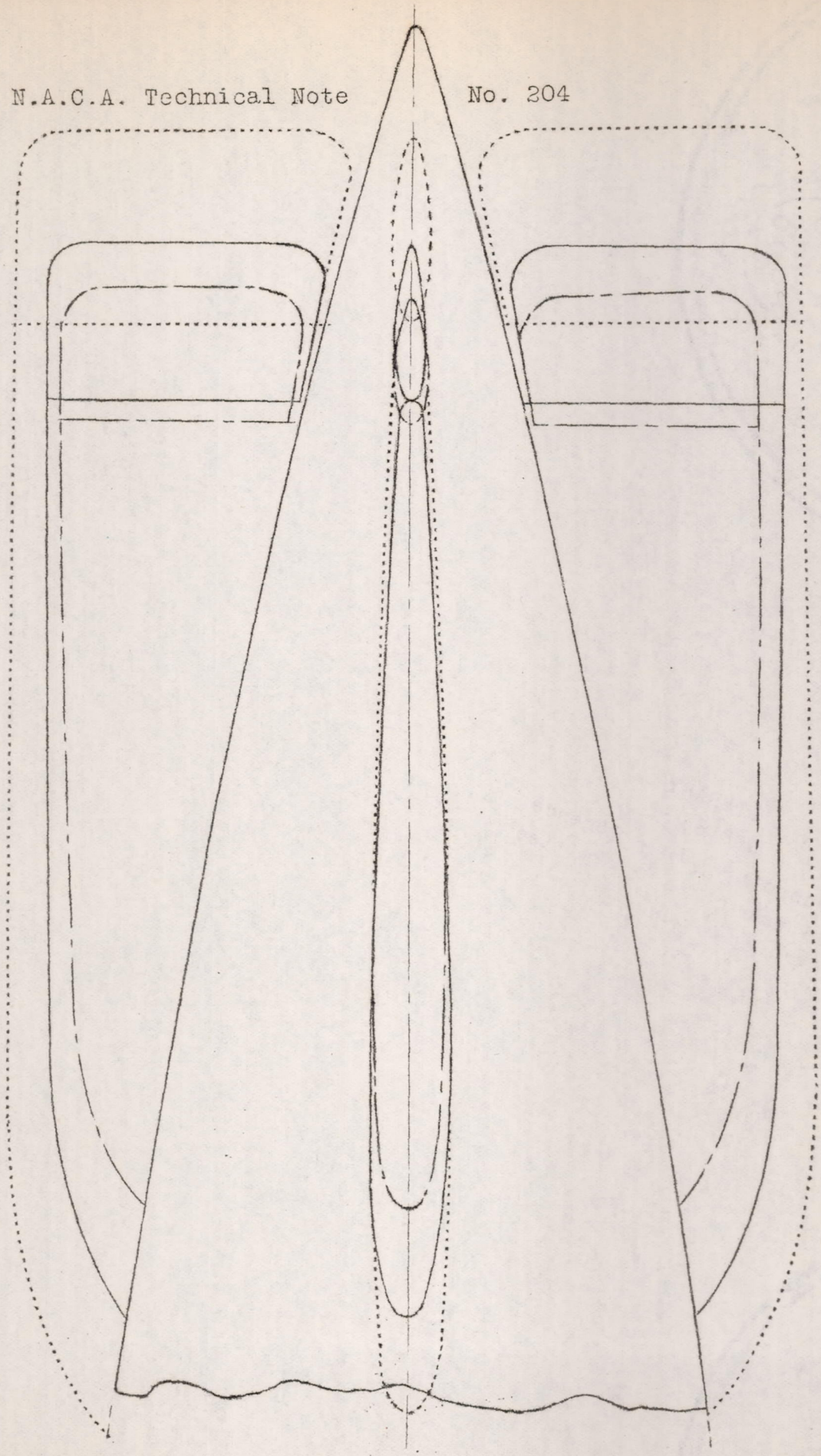

Full line denotes standard area
Dotted line " 150 % "
Dot & dash line denotes 75 % area

Fig. 9 Area group

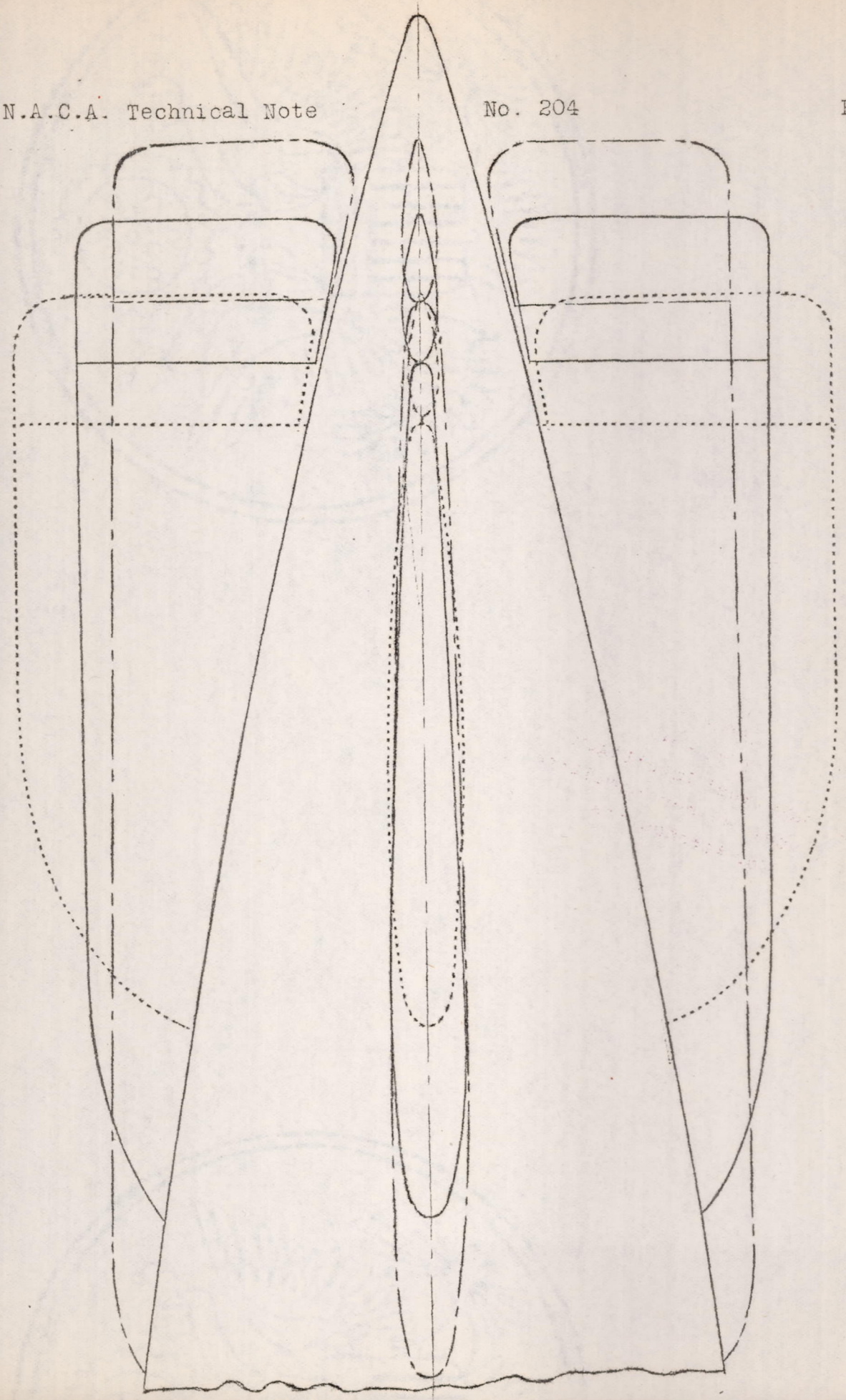

Full line denotes standard aspect ratio
Dotted line " 150 % " "
Dot & dash line " 75 % " "

Fig. 10 Aspect ratio group

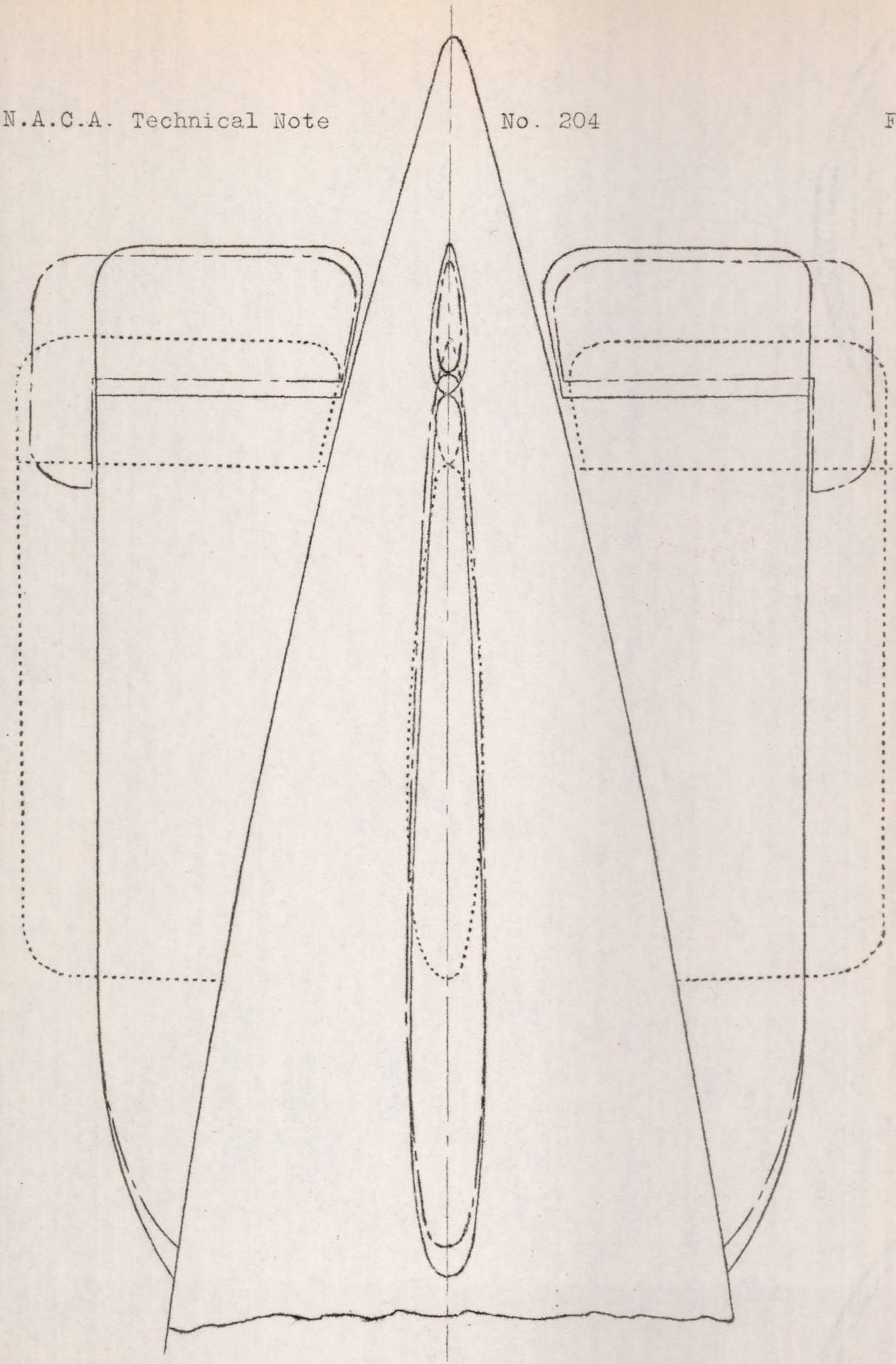

Full line denotes standard form
Dotted line " rectangular form
Dot & dash " balance rudder type

Fig. 11 Form group

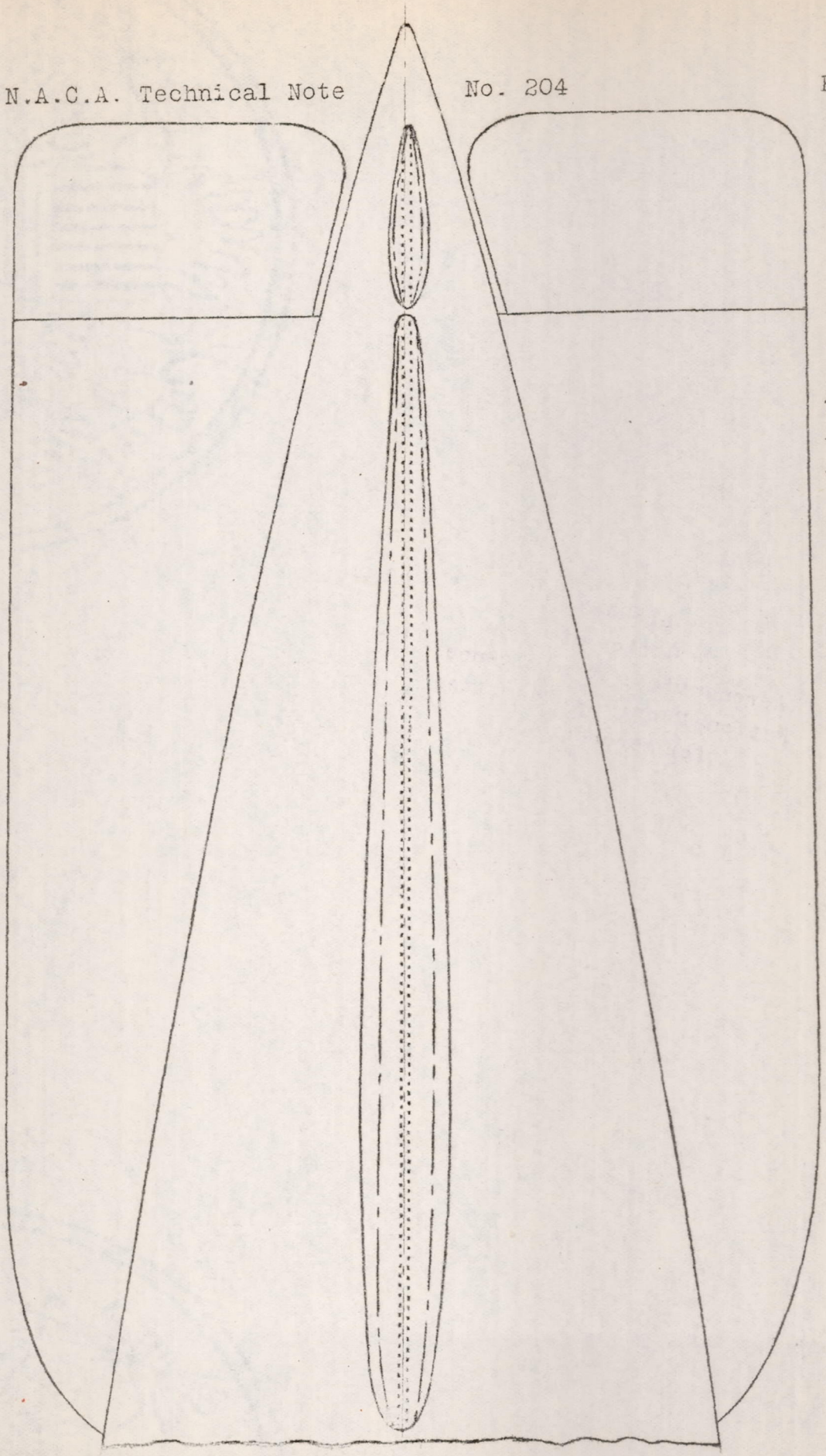

Full line denotes standard thickness (1/2")
Dotted line " 1/16" "
Dot & dash " 1/4" "

Fig. 12 Thickness group

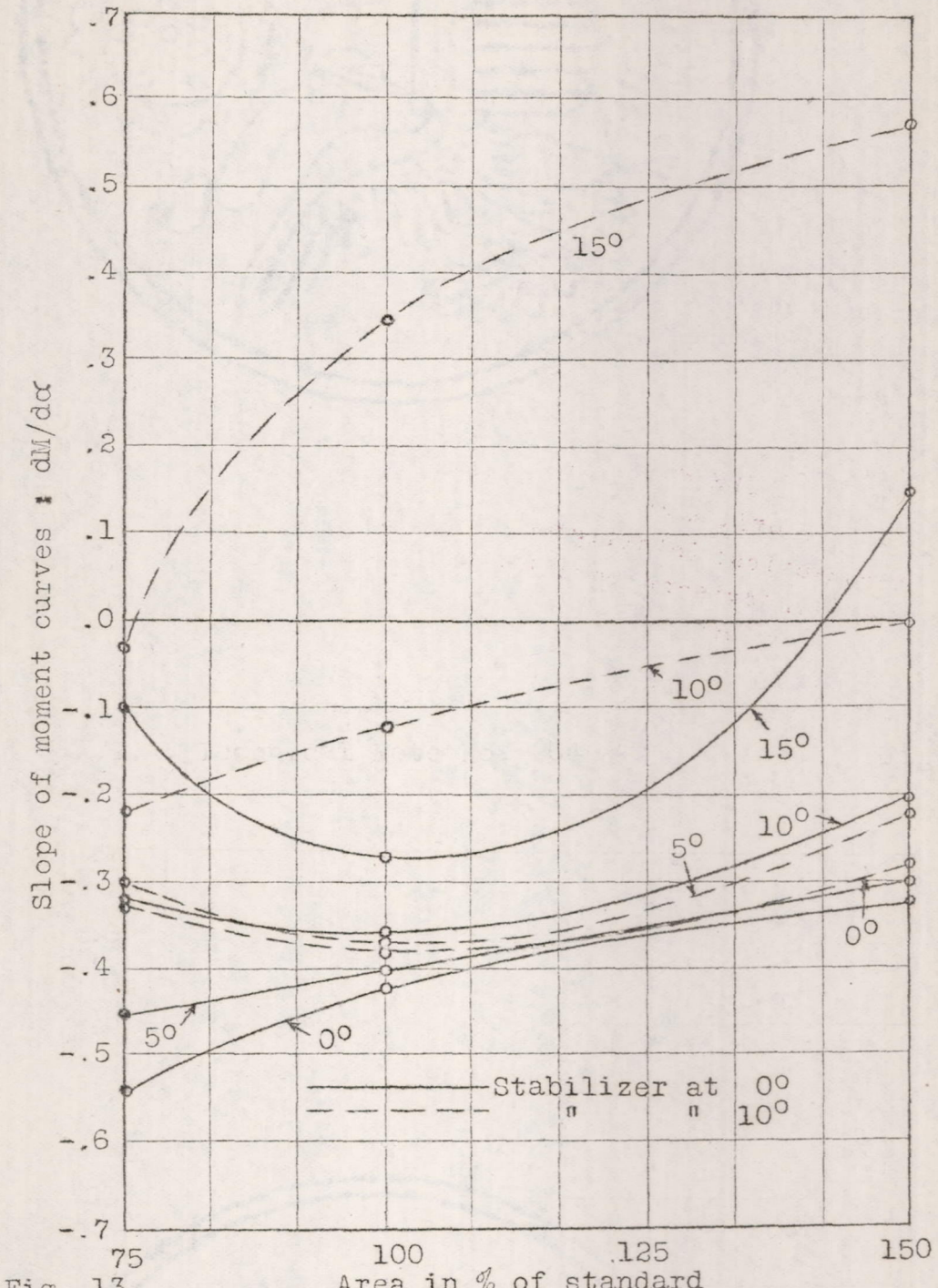
.7
.6
.5
.4
.3
.2
.1
.0
-.1
-.2
-.3
-.4
-.5
-.6
-.7
Slope of moment curves = dM/dα
15°
10°
15°
10°
5°
0°
5°
0°
Stabilizer at 0°
" " 10°
75
100
125
150
Area in % of standard

Fig. 13

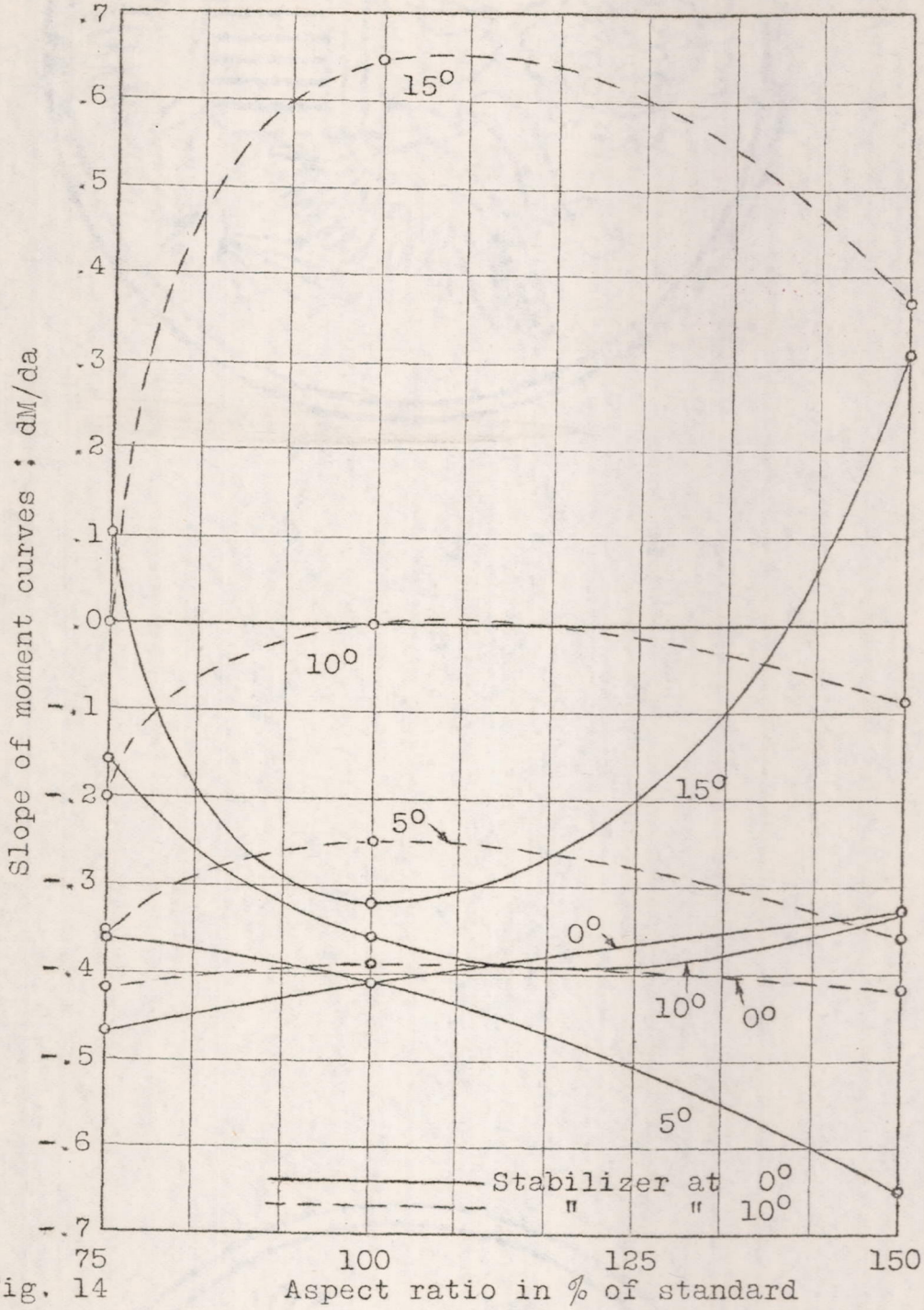
.7
.6
.5
.4
.3
.2
.1
.0
-.1
-.2
-.3
-.4
-.5
-.6
-.7
Slope of moment curves : dM/da
15°
10°
5°
0°
15°
10°
0°
5°
Stabilizer at 0°
" " 10°
75
100
125
150
Aspect ratio in % of standard

Fig. 14

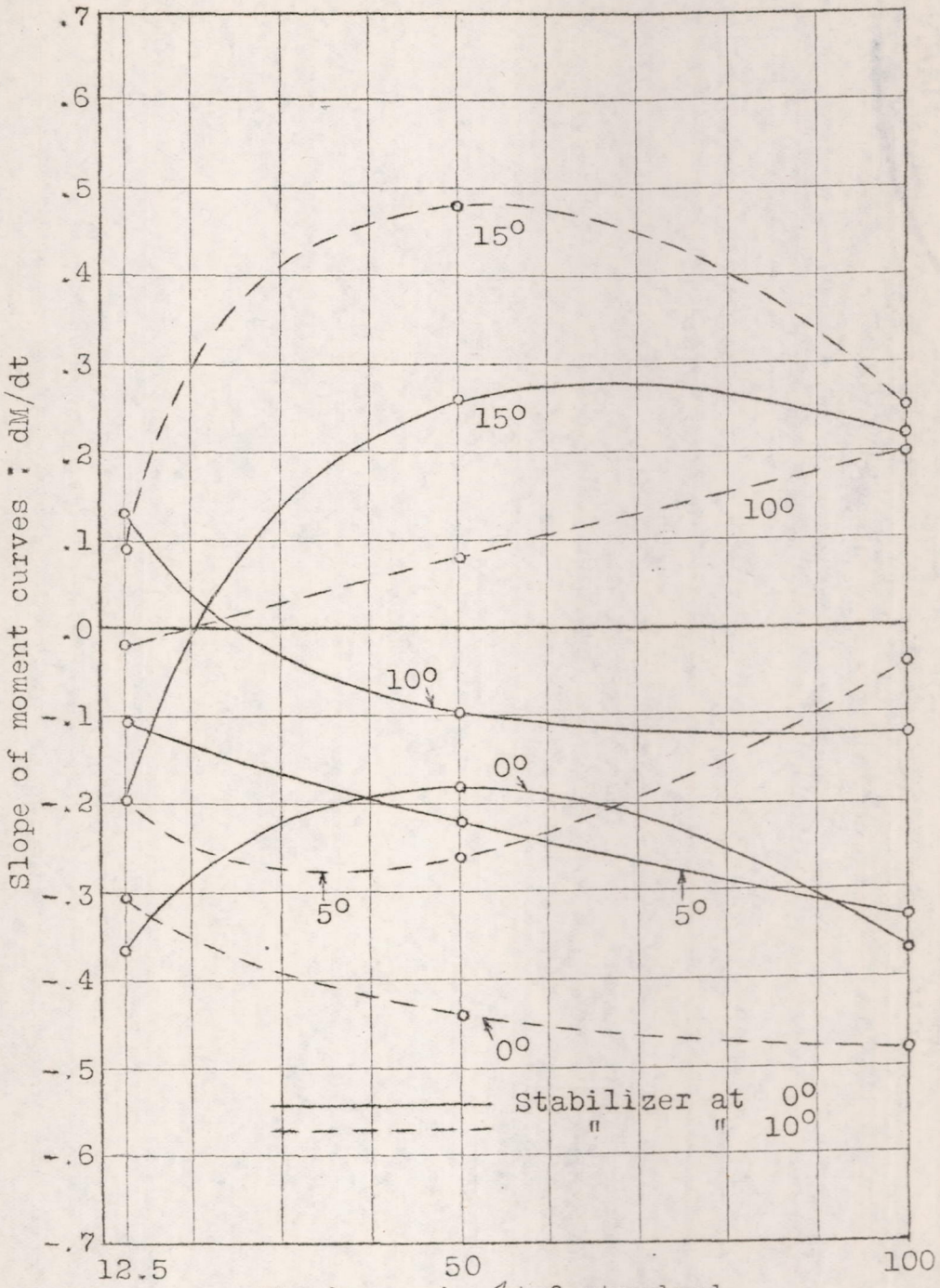
.7
.6
.5
.4
.3
.2
.1
.0
-.1
-.2
-.3
-.4
-.5
-.6
-.7
Slope of moment curves : dM/dt
15°
15°
10°
10°
0°
5°
5°
0°
Stabilizer at 0°
" " 10°
12.5
50
100
Thickness in % of standard

Fig. 15

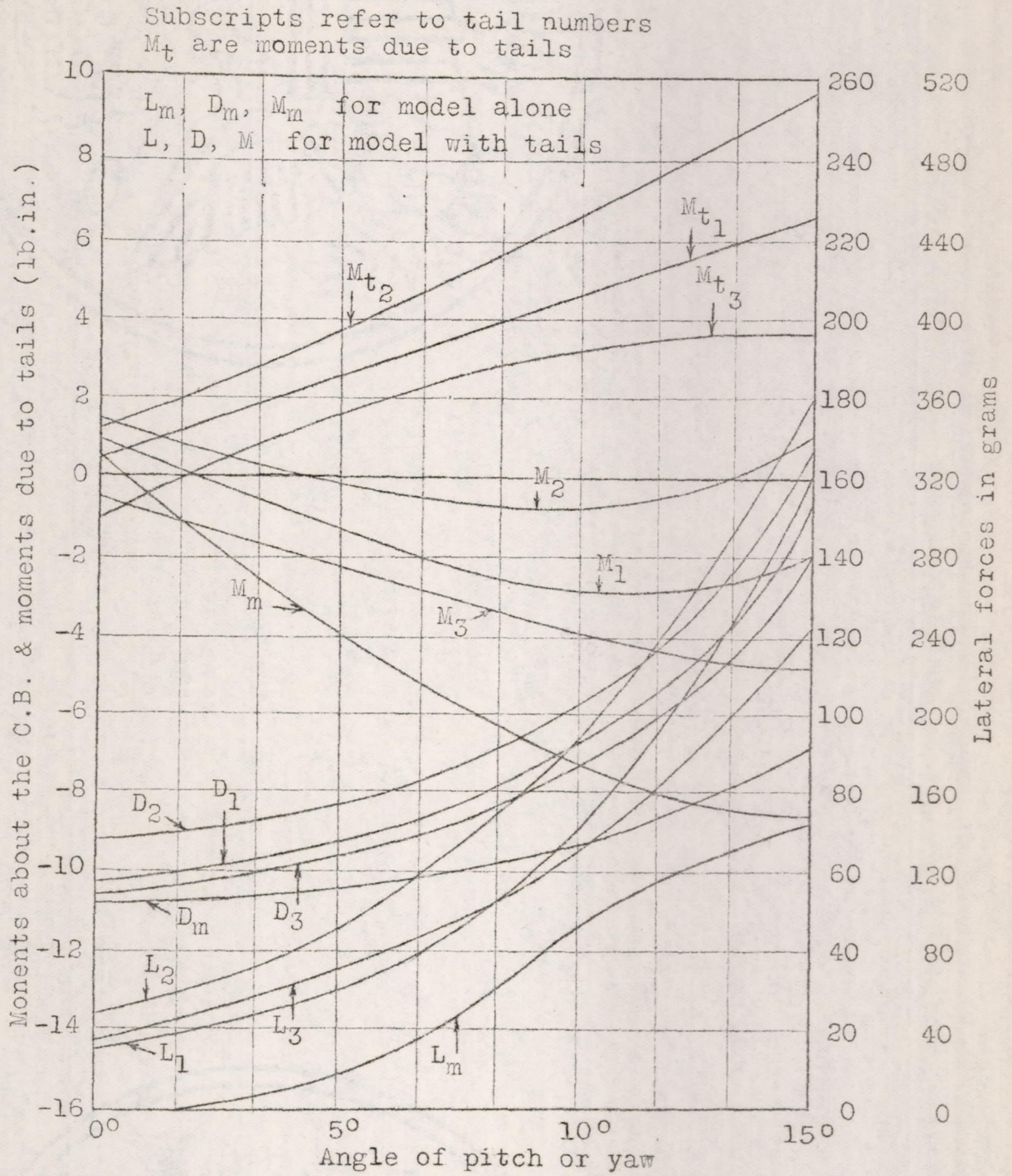

Fig. 16 Performance curves of an L-33 model fitted with area group of tail surfaces. Elevators 10°

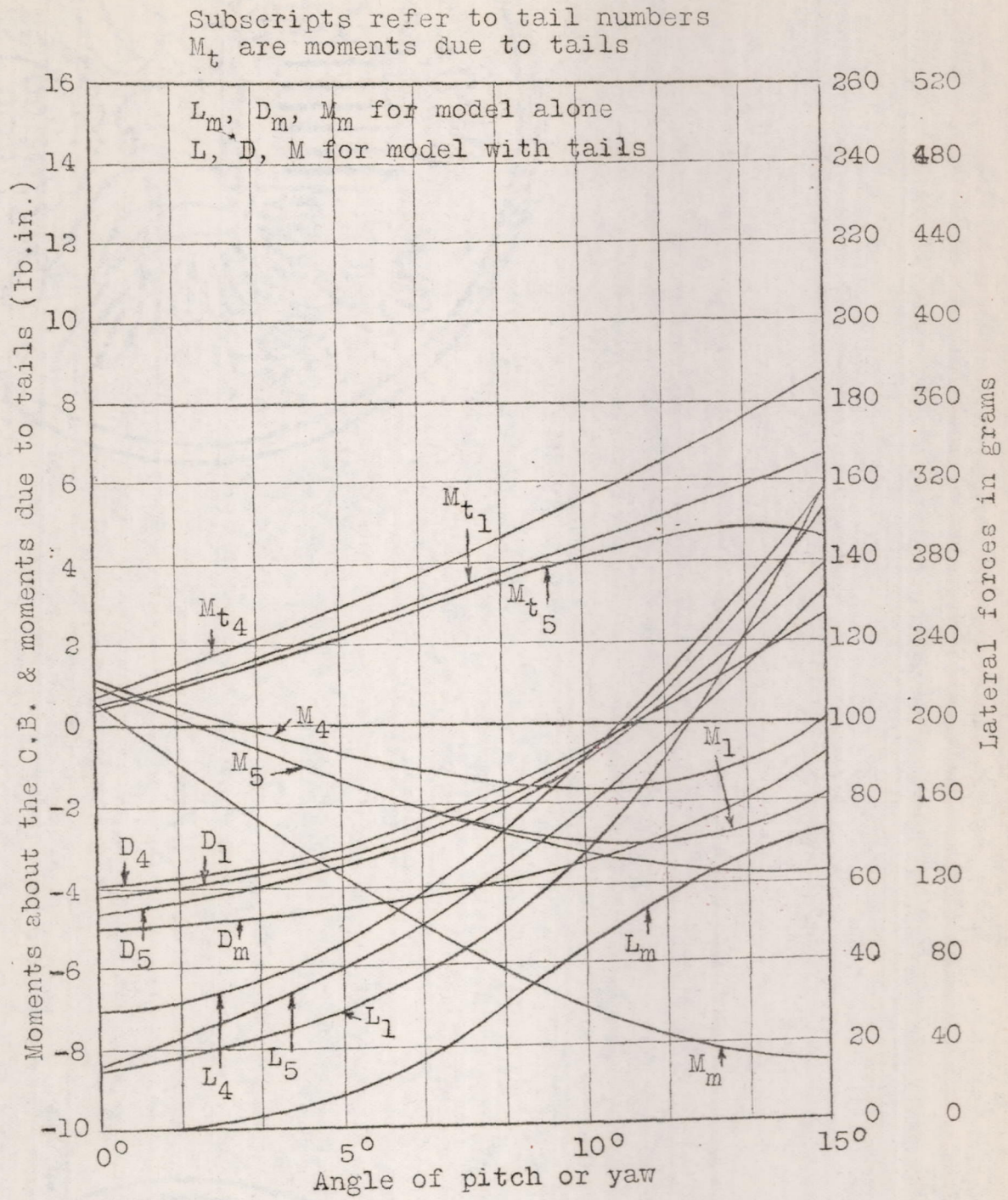

Fig. 17 Performance curves of an L-33 model fitted with aspect ratio tail surfaces. Elevators 10°

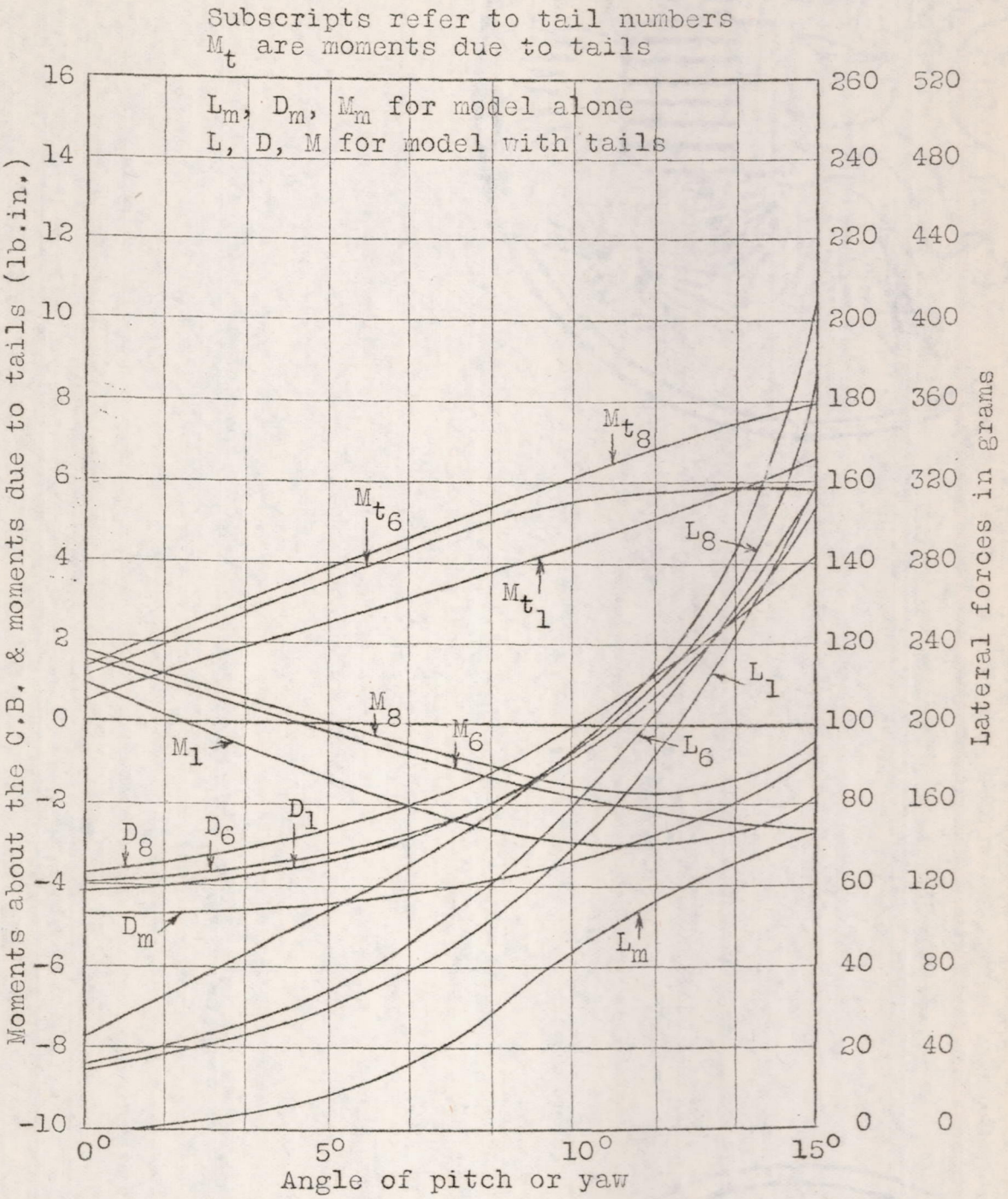

Fig. 18 Performance curves of an L-33 model fitted with form group of tail surfaces. Elevators 10°

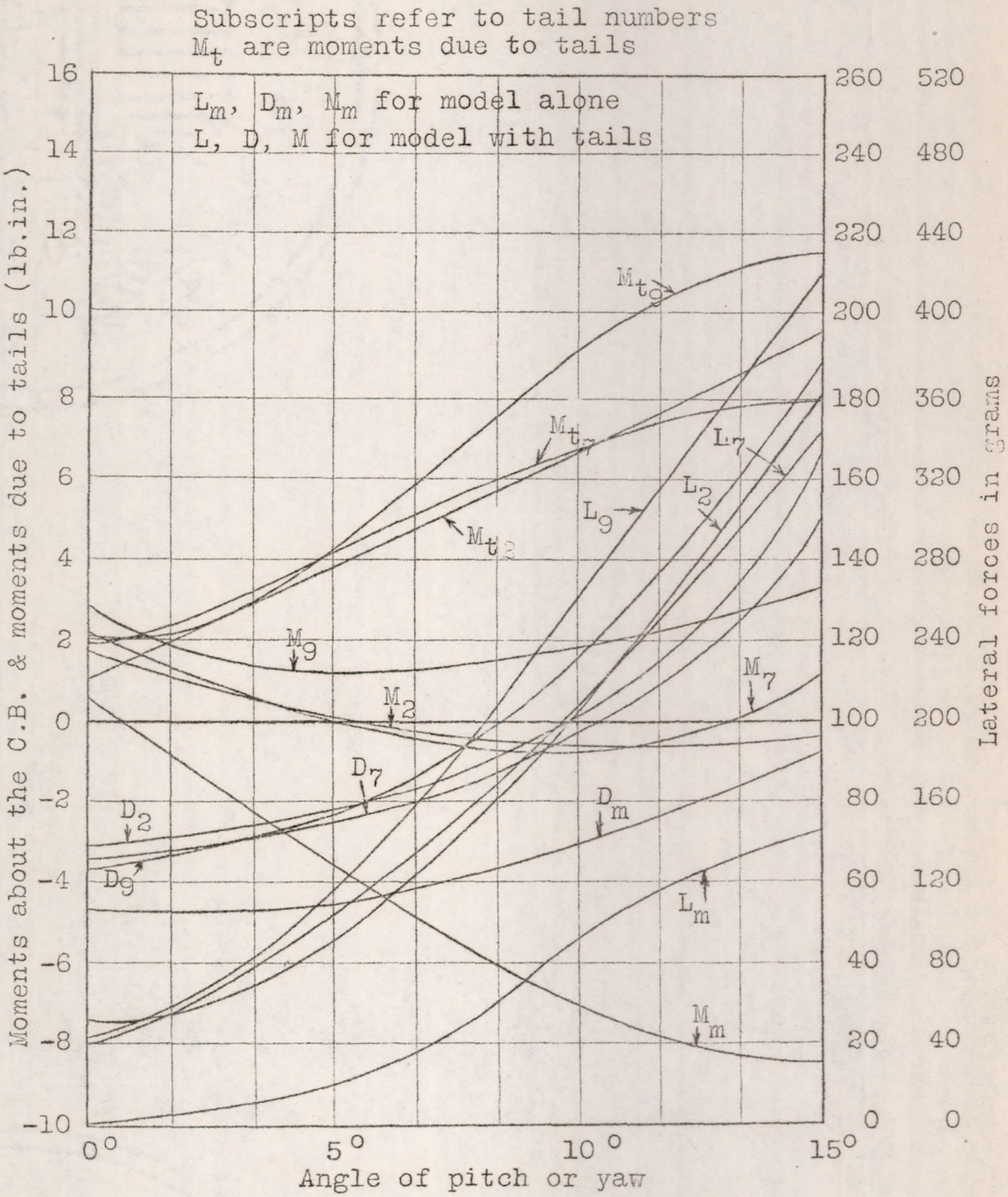

Fig. 19 Performance curves of an L-33 model fitted with thickness group of tail surfaces. Elevators 10°